Evolution of microstructure and correlation of Microstructure and Tensile properties of Inconel 718

A thesis submitted in fulfillment of the requirement for the degree of

Master of Technology

In

Material Engineering

Submitted by

TUHIN GHOSH

Examination Roll no. – **M4MAT19024**

Under the supervision of

PROF. P.C. CHAKRABORTI

Department of

Metallurgical and Material Engineering

Jadavpur University

Jadavpur, Kolkata-700032

Certificate

This is to certify that the thesis entitled **"Evolution of Microstructure and Correlation of Microstructure and Tensile properties of Inconel 718"** submitted by Mr. Tuhin Ghosh in fulfillment of the requirements for the award of the degree of Master of Technology in Material Engineering at Jadavpur University, Kolkata is an authentic work carried out by him under our supervision and guidance.

To the best of our knowledge, the matter embodied in the thesis has not been submitted to any other university/institute for the award of any degree or diploma.

Prof. P.C. Chakraborti
Thesis advisor
Department of
Metallurgical and Material engineering
Jadavpur University
Kolkata – 700032

Prof. A.K. Pramanick
Head of the Department of
Metallurgical and Material Engineering
Jadavpur University
Kolkata - 700032

Dr. S. Sivaprasad
Thesis co-advisor
Materials Engineering Division
National Metallurgical Laboratory
Jamshedpur

Prof. Chiranjib Bhattacharjee
Dean
Faculty council of Engineering and Technology
Jadavpur University
Kolkata - 700032

DECLARATION OF ORIGINALITY AND COMPLIANCE OF ACADEMIC ETHICS

I do hereby declare the thesis contents literature review and original research work by the undersigned candidate, as part of my Master of Technology in Material Engineering, studies during academic session 2018-2019.

All information in this document has been obtained and presented in accordance with academic rules and ethical conduct.

I also declare that I have fully cited and referred all the material and results that are not original to this work.

Name- **Tuhin Ghosh**
Exam Roll no- **M4MAT19024**
Class Roll no- **001711303025**
Registration no-**140915 of 2017 - 2018**

Signature----------
Date----------

JADAVPUR UNIVERSITY
FACULTY OF ENGINEERING AND TECHNOLOGY

CERTIFICATE OF APPROVAL

The foregoing thesis is hereby approved as a credible study of an engineering subject carried out and presented in a manner satisfactory to warrant its acceptance as a prerequisite to the degree for which it has been submitted. It is to be understood that by this approval the undersigned does not necessarily endorse any statement made, opinion expressed or conclusion drawn there in but approved the thesis only for the purpose for which it has been submitted.

Signature of the Final Examiners for Evaluation of Thesis along with the date.

- ----------
- ----------
- ----------

Acknowledgement

With deep regards and profound respect, I avail this opportunity to express my deep sense of gratitude and indebtedness to Prof. P.C. Chakraborti, Metallurgical and Materials Engineering Department, Jadavpur University for introducing the present research topic and for his inspiring guidance, constructive criticism and valuable suggestion throughout the research work. It would have not been possible for me to bring out this thesis without his help and constant encouragement.

I am sincerely thankful to Dr. Soumitra Tarafdar, Dr. H.N. Bar, Dr. G.V.S. Murthy, Dr. P. Munda and other faculty members of MTE department of NML for their persistent support and advice during the course work.

I am also highly grateful to laboratory members of Material Testing and Evaluation, NML jamshedpur, specially Mr. Hrishikesh Shastri, Mr. Rahul Chauhan, Mr. Lalit Gupta, and Mr. Amit Belung for their help during the execution of experiment.

Last but not the least, I wish to place my deep sense of thanks to my friends for their cooperation and critical suggestion during my project work and studies.

Contents

Chapter 2 – Literature review

Chapter 3 – Experimental work

Specimen designation

Specimen name	Specification
IN_{AR}	As received specimen
IN_0	Block solution annealed at 980°C
IN_1	Block solution annealed + heat treated at 650°C for 75 hours + soaked at 620°C for 8 hours
IN_2	Block solution annealed + heat treated at 750°C for 75 hours + soaked at 620°C for 8 hours
IN_3	Block solution annealed + heat treated at 800°C for 75 hours + soaked at 620°C for 8 hours
IN_4	Block solution annealed + heat treated at 900°C for 75 hours
IN_S	Block solution annealed + heat treated at 720°C for 8 hours + soaked at 620°C for 8 hours
IN_O	Block solution annealed at 1095°C then oil quenched
IN_F	Block solution annealed at 1095°C then furnace cooled
IN_W	Block solution annealed at 1095°C then water quenched
IN_1RT	Tensile specimen heat treated at 650°C for 75 hours + soaked at 620°C for 8 hours then tested at room temperature
IN_1HT	Tensile specimen heat treated at 650°C for 75 hours + soaked at 620°C for 8 hours then tested at high temperature (650°C)
IN_2RT	Tensile specimen heat treated at 750°C for 75 hours + soaked at 620°C for 8 hours then tested at room temperature
IN_2HT	Tensile specimen heat treated at 650°C for 75 hours + soaked at 620°C for 8 hours then tested at high temperature (650°C)
IN_3RT	Tensile specimen heat treated at 800°C for 75 hours + soaked at 620°C for 8 hours then tested at room temperature
IN_3HT	Tensile specimen heat treated at 800°C for 75 hours + soaked at 620°C for 8 hours then tested at room temperature (650°C)
IN_4RT	Tensile specimen heat treated at 900°C for 75 hours then tested at room temperature

IN_4HT	Tensile specimen heat treated at 900°C for 75 hours + then tested at high temperature (650°C)
IN_SRT	Tensile specimen heat treated at 720°C for 8 hours + soaked at 620°C for 8 hours then tested at room temperature
IN_SHT	Tensile specimen heat treated at 720°C for 75 hours + soaked at 620°C for 8 hours then tested at high temperature (650°C)

Abstract

This investigation examines the high temperature behavior and post tensile properties of forged Inconel 718 in solution annealed and variety of thermal ageing condition. Precipitation hardening is a phenomena of strengthening the material by the precipitation of major strengthening phases at high temperature to attain maximum strength properties. One set of Inconel 718 blocks were solution annealed by soaking the as received Inconel bar at 980°C for 1 hour prior to machining for microstructural analysis and other set were heat treated in a scheduled heat treatment temperature from 650°C to 900°C for 75 hours then soaked at 620°C for 8 hours followed by water quenching. Some specimens were undergone double ageing treatment which was carried out at 720°C for 8 hours followed by soaking at 620°C for 8 hours. The microstructural analysis were carried out with the help of scanning electron microscope and to get brief idea about the microstructural constituents EDS analysis were also performed. Hardness measurements were done by the help of a Vickers hardness tester by applying 30kg load with dwell time of 10 s.

Specimen for tensile test were designed with gauge diameter diameter of 6mm and reduced gauge length of 14mm. Strain controlled tensile test were carried out at room temperature as well as high temperature in servo-electric universal testing machine. The high temperature tensile tests were performed at 650°C and at constant strain rate of 10^{-3} s^{-1} by the help of a high temperature extensometer of gauge length 12.5 mm with 100% travel. Fractographic analysis were carried out on the fractured samples by using SEM.

The results highlight that the growth of major strengthening phases occurs in between 650°C - 750°C and these specimens possesses higher strength. At higher temperature the growth of stable grain boundary phases are also observed and precipitation of carbides at the boundaries as well as inter granularly. Though the double aged specimens have shown highest strength properties, at high temperature their ductility became poor. The fractography analysis show that dimple ruptures at lower temperatures and the decreasing size of the dimples with increasing temperature. Vicker's hardness test show that hardness decreases with increasing ageing temperature.

Key words: Inconel 718, precipitation hardening, solution annealing, double ageing, EDS, Fractography, grain boundary phases

List of figures

List of Tables

Chapter 1: INTRODUCTION

1.1 High temperature alloys

Literally high temperature alloys are those materials which can withstand a temperature of 500^0C or above. These materials possess a great ability to keep maintaining their properties at high temperature. High strength and stability as well as good creep, corrosion and oxidation resistance at higher temperature makes them exceptional from other materials. The base alloying element of a super alloy is mainly Ni, Co or Fe. Around 1940s iron based super alloys were used in enormous number then in late 1950s with the development of vacuum melting process fine control of the chemical compositions of the super alloys could be possible. The important characteristics that made super alloys effective in torturous or critical environment are –

I) Hot form and forge ability
II) Gamma prime and double prime
III) Responding well in heat treatment
IV) Oxidation and corrosion resistance
V) Able to be coated
VI) Achieving desirable grain structure by successive hot working

Among Ni, Co and Fe based high temperature alloys the Ni based alloy is used in a wide range. Ni based alloys are best known for their good resistance in static, fatigue and creep loading conditions in high temperature applications. Some examples of super alloys are – Nimonic 75, Nimonic 80A, Inconel 718, Inconel 625, Haynes 25, Haynes 282, Waspaloy, Nitronic 60. In this thesis our discussion will be bounded only in Inconel 718 and its properties, behavior at elevated temperature, microstructural constituents and mechanical testing results at room temperature and high temperature.

The various areas of application of super alloys are as follows-

i) It is used in thermal power plants in the steam turbine section, in making the blades, bolts and flue gas re-heaters.
ii) In gas turbine or aircraft system it is used in making turbine discs, casing shafts, blades, vanes, exhaust system etc.
iii) It is used in IC engines also, in the turbocharger part, hot plugs, exhaust valves.

iv) Its application is wide in rocket engine parts and aerodynamic equipment in space field.

v) It is used in medical apparatus such as prosthetic devices and as well as in pollution control devices such as scrubbers.

1.2. INCONEL 718

Inconel 718 is a Nickel based super alloy which possesses high strength and durability at high temperature and good creep resistance that makes them suitable for using in aerospace, aircraft and oil fields in a wide range. As it is useful in high temperature and it allows the engine to run continuously at that temperature it reduces the fuel consumption as well. The chemical compositions of Inconel 718 are as follows-

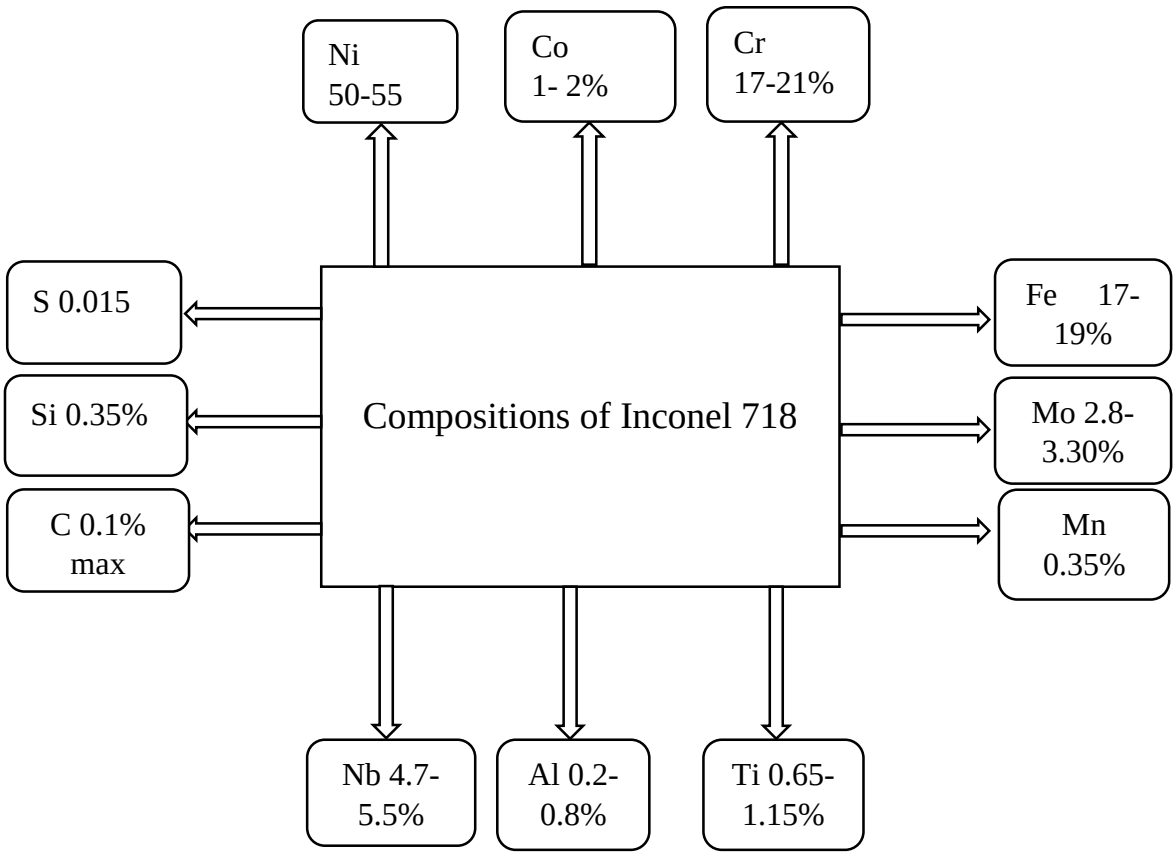

Ni based alloys are mainly single crystal super alloys which is essential for turbine blades. The reason for giving priority to single crystal alloys over poly crystal is their good fatigue and creep resistance property. Grain boundary sliding is a non- avoidable problem in creep. As

single crystals has no grain boundary, the effect of grain boundary sliding can be avoided by using single crystal alloys over poly crystal alloys. The reason behind their superior strength at high temperature is the precipitation of γ' and γ''. These materials has very slow kinetics, the different phases present in the alloy starts exposing their properties at high temperature. Hence heat treatment at different temperatures was also suggested by the experts. The various phases that exists in the INCONEL 718 alloy are γ phase, γ', γ'', δ, laves phase, sigma, μ, M_6C carbides. Among all these phase the main strengthening phases are γ' and γ'' phases.

1.2.1 Gamma (γ) phase

Gamma phase is the austenitic solid solution matrix phase in the nickel based super alloys with FCC (face centered cubic) crystal structure. The constituents of gamma matrix which takes part in solid solution strengthening are nickel, chromium, iron, molybdenum, titanium and aluminum. This is weaker strengthening phase with compared to gamma prime and gamma double prime.

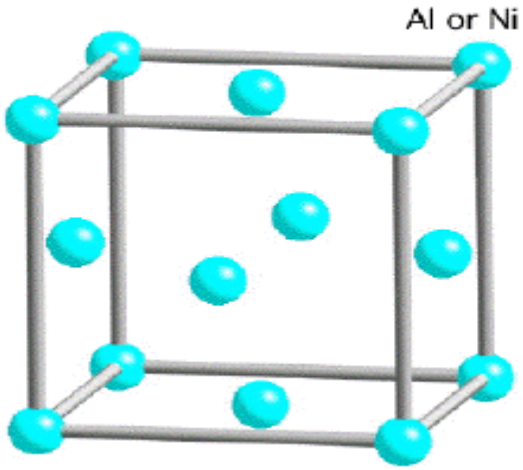

Fig 1. FCC crystal structure of gamma

1.2.2. Gamma prime (γ') phase

Gamma prime is an important strengthening phase in Inconel 718 alloy. It is an A_3B compound where A is mainly Ni and B is columbium with some amount of Ti and Al. It is not present in the alloy from beginning, it comes after proper heat treatment of the material considering the suitable parameters. It has also FCC crystal structure.

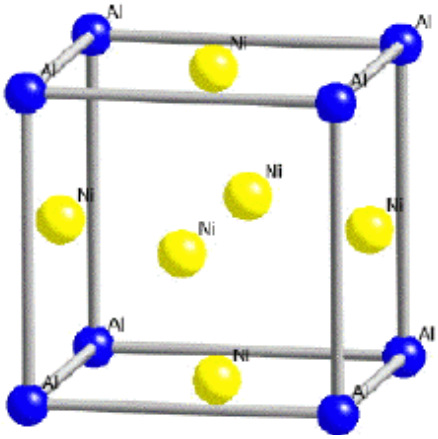

Fig 2. FCC gamma prime

Ni atoms are at the center of each faces while Al or Ti atoms are at the corners of the cube. Hence they form Ni_3Al or Ni_3Ti. Both the matrix phase and intermetallic gamma prime phase has FCC crystal structure but there is a slight change in the lattice parameter among these two strengthening phases which is not more than 5%

Based on the aluminum content in the gamma prime phase the yield strength increases accordingly with the increase of temperature within -160^0C to 800^0C. Though the constituents of gamma prime are only Ni, Al and Ti where Ni is in larger fraction, but Al and Ti can be replaced significantly by sufficient amount of Nb. Gamma prime particles are mostly spherical in shape and within the range of 50 Å to 2500 Å for INCONEL 718 but in some alloys such as Udimet-700, Mar-M200, Mar-M421 gamma prime precipitates show their cube shaped morphology.

1.2.3. Gamma double prime (γ'') phase

Gamma double prime is the main strengthening phase of Inconel 718 alloy. It has a BCT (Body Centered Tetragonal) crystal structure. It is a metastable Ni_3Nb phase which is of round particle shape having dimensions less than 200 A^0 at high temperature whereas in normal condition it possesses disk shape having length 5-6 times its thickness.

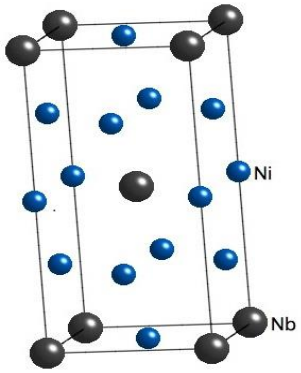

Fig 3. Gamma double prime BCT structure

Some of the important mechanical properties of Inconel 718 such as tensile and creep properties are controlled by the gamma double prime precipitate. During ageing the coarsening behavior of gamma double prime leads to give rise the delta phase. This phase becomes metastable above 650^0C.

1.2.4. Delta (δ) phase

Delta phase is a stable intermetallic Ni_3Nb phase which has orthorhombic crystal structure that contains very less amount of Nb as a constituent. Though it has similar intermetallic phase like gamma double prime, it contains only 5 wt% of Nb. It is not a strengthening phase in Inconel 718 alloy. Delta phase can be of needle like shape which forms in between 800^0C to 1100^0C along the grain boundaries.

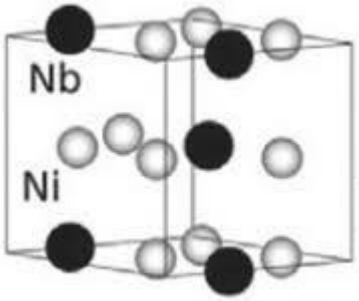

In Inconel 718 gamma double prime is main strengthening phase but the nucleation of delta phase helps in stabilizing the grain size and to improve the stress rupture behavior at high temperature. Delta phase starts forming at the expense of gamma double prime above 800^0C as gamma double prime starts coarsening after that temperature.

Fig 4. Orthorhombic Ni_3Nb (δ)

1.2.5. Laves phase

Laves phase is a Nb rich intermetallic phase with hexagonal closed packed structure in form of $(Ni, Fe, Cr)_2$ (Nb, Mo and Ti). This phase consume a greater amount of Nb that is the main requirement for the strengthening of Inconel 718 alloy by forming gamma double prime precipitates. Laves phase can be of round particle shaped which mainly forms in the segregated region. After aging treatment during solidification laves phase forms at low temperature inter-dendritically in the segregated areas. Laves phase is brittle in nature and hence it leads to decreasing ductility and creep properties. It is necessary to minimize the formation of laves phase due to its detrimental effect on tensile and creep properties of the material.

1.2.6. Carbides

The formation of metal carbides occurs due to the reaction of constituents like Ti, Hf, Ta, Cr, Mo with Carbon. Some carbides in the form of MC, M_6C, $M_{23}C_6$ where M stands for Cr, Ti, Ta, Mo are formed during aging in the inter-dendritic regions. Among these carbides $M_{23}C_6$ forms at lower temperature around 750^0C. Carbide phase can show both morphologies globular and blocky. Carbide phase consumes Nb in large amount which is a much needed element for the precipitation of gamma double prime during strengthening. If the heat treatment

temperature increased the formation of carbides may be reduced but due to the stability of the material at high temperature some amount of carbides still can be observed.

1.2.7. NbC and TiN phases

TiN phase forms during solidification. As it forms in little amount hence this phase which is angular in shape is not a major concern in Inconel 718 alloy. Though this phase is stable up to the melting point.

Whereas NbC phase is not as stable as TiN phase but it forms in larger amount with compared to TiN phase. It also has angular shape. When annealing is done above 1038^0C this phase starts to dissolve and it precipitates in grain boundary as a film during aging between 704^0C to 982^0C.

1.3. Solution Annealing

Inconel 718 is mainly hardened by secondary precipitates such as gamma prime and gamma double prime in the metal matrix gamma. The main aging constituents such as TI, Al and Nb which plays important role in forming the secondary phases should be dissolved properly in the metal matrix. If these constituents precipitate in different manner or combined together and forms separately then precipitation will not be correct which will affect the strength properties of the material. So, to get all the strengthening phase dissolved in the matrix material, the material must be undergone solution heat treatment or solution annealing. It is done at 1700-1850^0F for 1 hour duration then rapid solidification by water to stop the growth of the precipitates.

1.4. Double aging technique

After solution annealing different heat treatment processes are performed taking in consideration different service condition of the material. Double aging is an important technique which produces fine and homogeneous grains, improves ductility and causes high strength and good low cycle fatigue properties. Double aging resists the growth of cracks in grain by forming δ phase which will later be precipitated along the grain boundary and will restrain the growth of crack. Gamma prime is an effective strengthening phase in Inconel 718 and precipitation of this phase occurs effectively in double aging rather than single aging. In

this process gamma prime precipitates in much larger amount to increase the strength of the alloy.

1.5. Metallography

Metallography involves in the structural study of the metal and its alloys by examining the specimen using microscope. Basically three types of microscopes are widely used to perform the examinations, those are Optical microscope, Scanning Electron microscope, Transmission Electron microscope. The useful information that we get from this are- about the microstructures of the different phases and their morphologies, chemical compositions of the phases. Before performing the examination in microscope the material must be undergone some basic process to prepare the sample such as mounting, paper polishing, cloth polishing, etching, ultrasonic cleaning. The processes are described below in brief-

1.5.1. Mounting

For small specimens mounting is required to hold the sample. Basically mounting is done by placing the sample into a mould and filling it with suitable material then applying pressure by mounting presses on it that will result a strong hold into it during operation in belt grinding or mechanical polishing. Bakelite, copper can be used as mould material. Two types of processes are there for mounting of the specimen – a) Hot mounting (in this process the synthetic powder material liquefies and with applying heat and pressure it gets embedded with the specimen.) b) Cold mounting (can be done using synthetic resins such as- polyester, epoxy resins)

1.5.2. Grinding and Polishing

After mounting is done, to make the surface of the block flat grinding must be done using silicon carbide papers. The grit size may vary from 120 to 2000. To get flat surface the block must be rubbed along forward and backward direction of the paper repeatedly until uniformly fine surface obtained. After performing grinding in one paper next grade of paper is taken and the sample after washing with water it should be hold rotating in 90^0 angle than the previous. The same process will be repeated while using the other emery papers of different grades. The grinding operation must be carried on to make sure that no scratches are left on the surface of the material.

After grinding to an extent the sample must be undergone cloth polishing which is done in a cloth polishing machine using a diamond impregnated cloth and a mineral oil as lubricant. Size of the diamond abrasives may vary from 0.25μm to 6 μm. The operation is carried out holding the mounted sample on the rotating cloth by applying pressure. If the pressure is too little the rate of polishing will be lower and pits will start to come. But too much pressure can also cause the distortion of the metal surface. So, pressure should be applied taking in consideration the hardness of the material.

1.5.3. Etching

Etching is necessary to obtain the structural development of the material sample which is to be examined in a microscope. But before etching, the sample should be cleaned of oil, other particles which got attached during polishing. The etchant mainly attacks on the boundaries by which the grains are separated from each other to distinguish the grains and to study their shape, orientation. After preparing the etchant the sample kept immersed in that for some time then it is dried by hand drier. As the etched surface is very reactive, it should kept in sealed desiccator and not be kept in air or touch by hand.

1.5.6. Optical Microscopy

Optical microscopy or light microscopy is used to observe the microstructure of the material surface after etching with proper etchant. It works on the principle of diffraction of light. The light source in optical microscopy is a lamp of tungsten filament. A condenser lens is used in between light source and specimen to focus the light rays on the specimen. The specimen is kept on the slide. There is another lens called objective lens of 10X-100X magnification which collect the diffracted rays from the specimen. Some additional magnification can be achieved by the eyepiece lens of 10X magnification. That implies, if we are observing a sample with 50X in objective lens, the optical microscope shows us the sample with magnification 500X ($50X \times 10X$). There are two different mode of visualization of the object in optical microscope, those are – a) Dark field microscopy and b) Bright field microscopy.

1.5.7. Scanning Electron Microscopy

Scanning Electron Microscopy deals with producing image of the sample by scanning its surface which is carried out with the help of a focused beam of electron on the material surface. The information that it provides are the topography or texture of the sample, about the

microstructure, their shape, composition of the microstructure and their amount and lastly the arrangement of the atoms in the object.

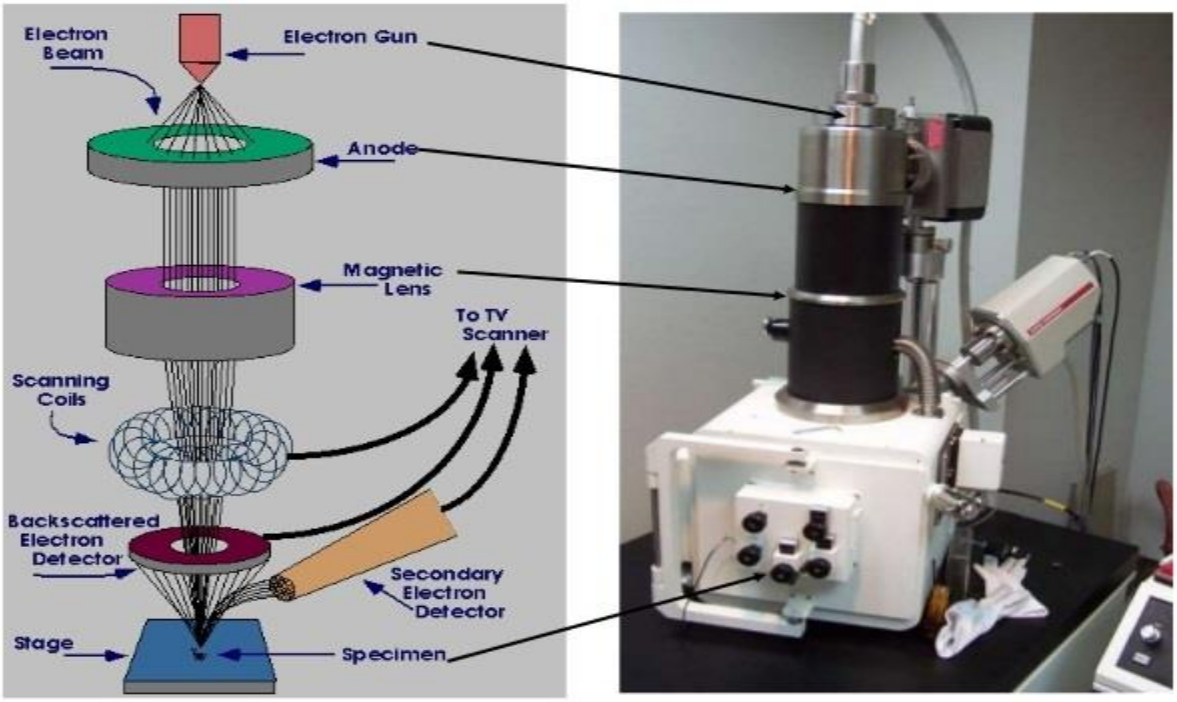

Fig 5. Schematic of scanning electron microscope

The main components of a scanning electron microscope are electron gun, magnetic condenser lens, scanning coils, vacuum system and detectors such as secondary electron detector, backscattered electron detector. From the electron gun a beam of electron emits and it passes through the anode to gain energy and then passes through the magnetic lens. The magnetic lens is used to collect the emitted electron beam and create an electron probe which is to be focused on the specimen. When the surface of the specimen struck by the electron beam, from each point signal comes out as electromagnetic radiation. There are detectors which collects the significant portions of the radiation such as Secondary Electron and Backscattered Electron. Then the detectors amplifies and displays these signals on the Computer monitor's screen.

1.5.8. Transmission Electron Microscopy

In transmission electron microscopy (TEM), image formation occurs by the transmission of electron beams through a specimen. In this case the specimen should be thinner than the previous. Operating principle of TEM is same like light microscopy but here electrons are uses instead of light due to their smaller wavelength and greater frequency. Hence the magnitude of

resolution attained by TEM is much better than the light microscope which helps in achieving the finest details of the structure of the specimen.

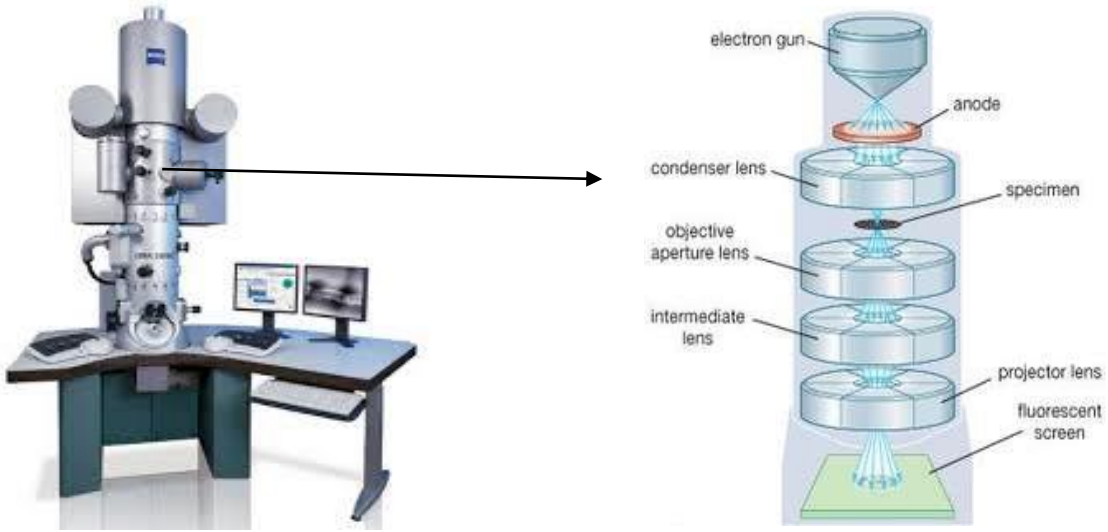

Fig 6. Schematic of transmission electron microscope

Electron beam is emitted from the electron gun and then they passes through a condenser lens which is kept there to focus them into a thin, coherent beam. After striking the specimen transmission of electron starts which highly depends on the transparency and thickness of the specimen. There is a phosphor screen where the image will be formed by the transmitted beam by the objective lens. The contrast of the image can be intensified by blocking out those electrons which diffracted at high angle using objective apparatus. There will be both dark and bright areas in the formed image where the dark areas will specify those places where transmission of electron is less and the bright areas will indicate the high electron transmission zone.

1.5.9. Energy Dispersive Spectroscopy (EDS)

Energy Dispersive Spectroscopy reveals what elements are there in the microstructure and composition or in short chemical characterization. It works on the phenomenon of characteristics x-ray spectrum emission. A high energy electron beam is charged onto the specimen being studied. The incident electron strikes on one of the inner shell electrons and knocks it out creating a vacancy there. Then, to fill that vacant position an electron from outer

shell jumps there and the energy difference between inner and outer shell releases as x-ray spectrum. An Energy Dispersive Spectrometer is there to detect this x-rays. After detection of those x-rays a pulse processor collects those signals and measure them then send to the analyzer to analysis of those information.

1.6. Vickers hardness test

Vickers hardness test deals with the indentation of the test specimen by the use of a diamond indenter which is shaped like a right pyramid with a square base and its angle between opposite faces are 136^0.

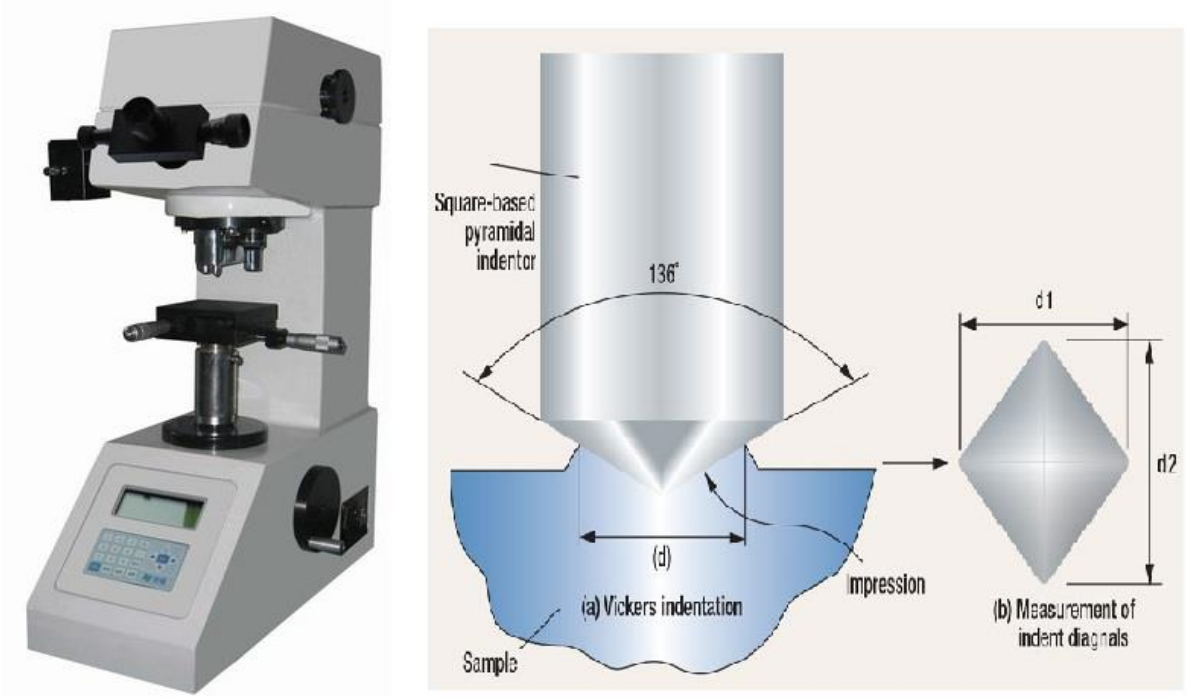

Fig 7. Vicker's hardness tester with diamond indenter

The load is applied normally for 10s to 15s. After indenting with the indenter the two diagonal length of indentation is measured using a microscope and then their average is calculated. Vickers hardness is calculated by dividing the applied load by area of indentation.

Chapter -2
Literature review

2.1. Metallurgy of INCONEL 718

Inconel 718 is a nickel based super-alloy which is well known for high temperature application. Basically Ni – based super alloys can be categorized in three groups- i) solid solution strengthened alloy (HAYNES 230), ii) precipitation hardened alloy (INCONEL 718) and iii) oxide dispersion strengthened alloy (Y_2O_3). Solid solution strengthened alloys mainly contains Fe, Al, Mo, Cr, Co, W these elements among which Mo, W, Al these are main strengthening elements which makes solid solution with Ni. Precipitation hardened alloys contains Al, Ti, Nb and Ta as their main strengthening elements. Presence of These elements in the alloy results in the formation of γ' and γ'' in the γ matrix. From several experiments it is evident in the below figure [1,2] that precipitation hardened material has greater strength in compare with solid solution hardened alloys and they are suitable for use in high temperature applications.

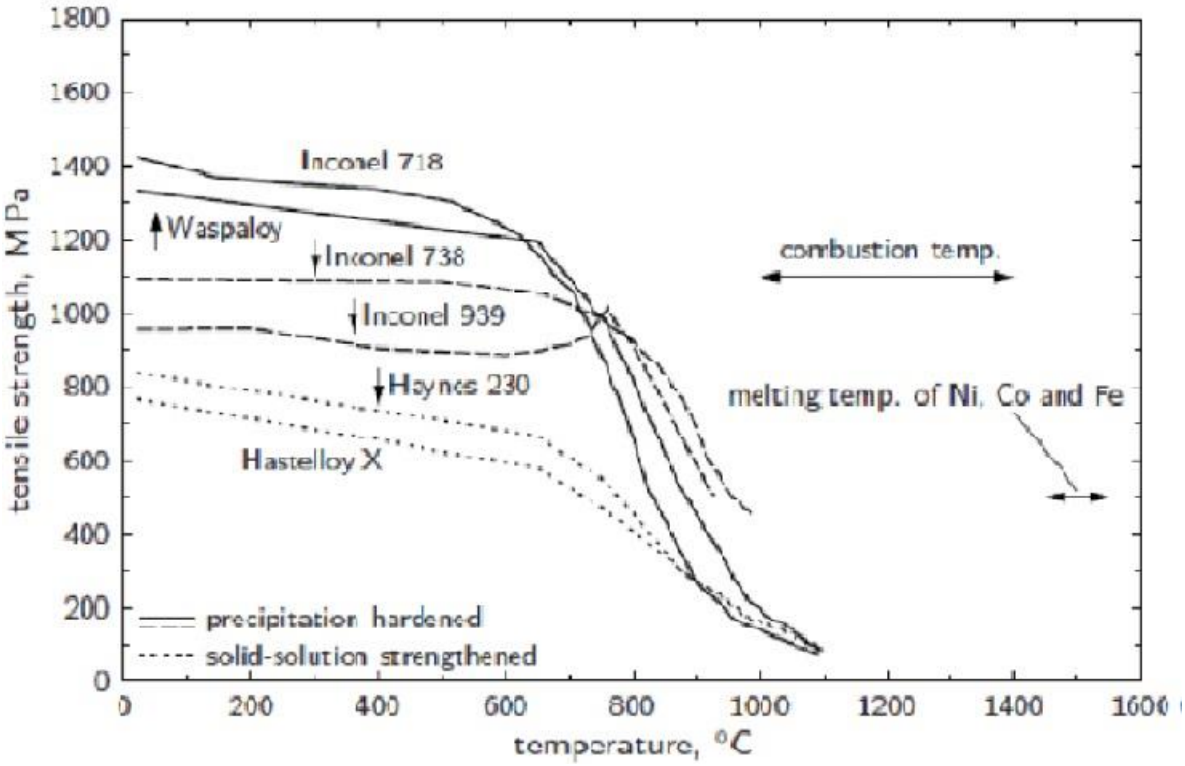

Fig 8. Variation of tensile strength with temperature of different Ni-base alloys

The microstructure of Inconel 718 consists of some strengthening phases such as gamma, gamma prime, gamma double prime and delta phase that precipitates over the matrix material due to ageing at different temperature and exposure.

2.1.1. Strengthening of Inconel 718 by precipitation hardening

Inconel 718 is strengthened by precipitation hardening or age hardening. The concept of precipitation hardening came in 1919 at International Nickel Company's research laboratory in Bayonne where the age hardening was first performed on Monel 400 alloy [3]. The high temperature strength and good mechanical properties are achieved by some strengthening phases which comes accordingly with proper heat treatment. Primary strengthening phase for Inconel 718 is the γ'' phase that has a body centered tetragonal unit cell and having a composition of Ni_3Nb. One example of γ' strengthened super alloy is Waspaloy and Inconel 706 and Inconel 909 are those Ni based super alloy which is strengthened by both gamma prime and gamma double prime [4,5].

2.2. Precipitation of different phases in Inconel 718

The second phases such as delta phase, various carbides, laves phase of Inconel 718 are formed as solid stated compounds which has an ordered arrangement of different crystal structure or arrangement of atoms unlike the solid solution where the solute atoms are distributed randomly over the matrix. In other way they are termed as intermetallic [6]. Those inter-metalics such as delta or laves phases precipitates are hard and brittle in nature because of the ionic bonding of the intermetallic compounds where there is huge difference between the electronegativity of solute and solvent metal. But despite having such drawbacks these intermetallic phases exhibits high strength, good creep properties at high temperature. Apart from these there are main strengthening phase gamma prime and gamma double prime. The chemical composition of the alloy 718 plays a vital role in the formation of different strengthening phases.

2.2.1 Ternary phase diagram of Ni-Al-Ti

From the phase field of γ and γ' in the Ni-Al-Ti ternary phase diagram it is shown that- for a given chemical composition with increasing temperature fraction of γ' decreases. During solution annealing this phenomenon can be used where it is required to dissolve all the γ' phase in the gamma matrix at high temperature and then ageing treatment at lower temperature which will give rise to the strengthening precipitates and a uniform dispersion of those fine particles.

From the ternary phase diagram of Al-Ni-Ti, the phase boundary of (γ + γ')/γ' indicates that the phase is not totally stoichiometric [7]. The reason behind this might be the extra number of vacancies on the sub-lattices due to which the stoichiometric deviation takes place. Due to the similarity between the lattice parameters of gamma and gamma prime they are coherent when the size of the precipitates are small.

2.2.2 Lattice misfit

The strengthening properties of INCONEL 718 mostly depends on the coherency of gamma and gamma prime. After quantifying this coherency it is termed as lattice misfit δ. Higher the coherency smaller the lattice misfit.

$$\delta = 2 \times \frac{a_{\gamma} - a_{\gamma'}}{a_{\gamma} + a_{\gamma'}}$$

Where α_{γ} and $\alpha_{\gamma'}$ are lattice parameters for gamma and gamma prime. The misfit is positive when gamma prime has larger lattice parameter than gamma. A small lattice misfit leads to cubical gamma prime precipitates with sharp corner, which is a desirable thing for gas turbine blade components [5]. This misfit between gamma and gamma prime can be controlled by altering the chemical composition of the alloy, particularly the Al/Ti ratio. Whereas a negative misfit stimulates the formation of rafts in gamma prime, essentially the layers of the phase which is in perpendicular direction to the applied stress.

2.2.3. Strengthening by gamma prime

Gamma prime is an important microstructural constituent in Ni- based super alloys. It has FCC crystal structure which does not vary much from the gamma matrix. This kind of coherency and similarity results in high source of strength of the alloy. In optical microscope it is seen that fine gamma prime precipitates are distributed over the microstructure [8]. The rate of precipitation of gamma prime is so rapid that even water quenching can't prevent the formation of this phase. The range of temperature within which gamma prime will be formed varies accordingly with the compositions of the alloy. Depending on the time of exposure in high temperature it is evident that gamma prime starts forming at around 650^0C. While observing through electron microscope gamma prime seems like cubical shape or spherical and

sometimes looks like rough flagstone [8]. Gamma prime exhibits classical precipitation kinetics which starts with initial nucleation followed by growth which occurs at the grain boundaries but in general the majority precipitates homogeneously as uniformly distributed fine particles throughout the gamma matrix. The gamma prime structure is crystallo-graphically coherent with the gamma matrix and this advantage assist easy nucleation and stops excessive coarsening of the particles. One of the most favorable characteristics of gamma prime is that the high volume fractions which is up to 50% depending upon the composition of the material [9].

2.2.4. Coarsening of γ' (Rafting) in INCONEL 718

Coarsening of gamma prime phase under the influence of applied stress at high temperature is termed as rafting. This phenomenon affects the creep resistance of the material and it help determining the lifetime performance of turbine blades in aerospace industry [10]. At the time of coalesce of gamma prime, they form long range interconnected rafts. There are two types of rafting behavior that has been observed [11] –

i) n-type rafts in which gamma prime coarsen along the normal direction of applied stress. This type of rafts are responsible for plate like morphology of gamma prime.
ii) p-type rafts in which gamma prime coarsen along the parallel direction of applied stress. This type of rafting is responsible for rod like morphology of gamma prime.

2.2.5. Strengthening by gamma double prime

γ'' (gamma double prime) is a metastable phase (Ni_3Nb) with tetragonal space centered crystal structure (DO_{22}) . The gamma double prime precipitates has disc shaped morphology with the orientation relationship with gamma matrix $(001)\gamma \parallel \{001\}\gamma$ and $[100]\gamma \parallel \{100\}\gamma$. In the crystal structure of gamma double prime Ni and Nb combines to form BCT structure in the presence of Fe which acts as a catalyst. As the volume fraction of γ'' is greater with compared to gamma prime, the contribution of gamma double prime precipitates in strengthening the alloy is way more than that of gamma prime [12]. The three main factors on which the strengthening effect of gamma double prime relied on are as follows-

I. High coherence of the precipitates with the matrix or coherency strain between gamma double prime and the gamma matrix.
II. The smaller size of the precipitates.

III. The twining ability of the precipitates.

The twinning ability of the precipitates depends largely on their sizes. They can only twin below a critical size. When they exceeds this critical value the deformation mechanism changes to simple shearing phenomenon of the precipitates by pair of dislocation which is vastly known as dislocation shearing mechanism in γ'' at elevated temperature [13]. One of the factors, coherency hardening by gamma double prime precipitation is considered as the primary reason for strengthening in Inconel 718. It is reported that while undergoing heat treatment process at 1400^0F the precipitation of gamma double prime is most likely to occur in the Nb rich areas in a quick manner. But the precipitates in this case will have smaller size in compared to the gamma double prime formed during heat treatment at 1600^0F [14, 17].

2.2.6. Role of ''Nb'' in precipitation hardening

Niobium is present in Inconel 718 as one of the microstructural constituent in smaller amount but the contribution of Nb in strengthening mechanism is significant. Being one of the major refractory element and most electropositive among Ta, W and Mo which are used in super-alloys in various application it has strong affinity for the A_3B type topologically closed pack phase. In γ' (Ni_3Al) Nb substitutes for Al as does Ti. Nb is responsible for the formation of γ'' or Ni_3Nb, the BCT structured strengthener phase in Inconel 718 [15, 21]. In nickel based super-alloys gamma double prime become a superior contributor to the strength due to the presence of Nb in it. A slight raising in Nb content will enhance the strengthening stability of γ'' precipitation. Being a hardening element the excessive amount of Nb will lead to brittleness of the material. Then further addition of Ni will be required for further precipitation [16]. With increasing the Nb content in the alloy, presence of other undesirable phases such as laves phase forms. It is reported that above 5%, Nb is strongly responsible for the formation of laves phase and delta phase in the alloy 718 and shows its detrimental effect to both strength and toughness [17]. During solidification in both solid solution strengthened and precipitation hardened super alloy Nb tends to segregate in the inter-dendritic region. In most of the nickel based super alloys at the end of the solidification process the formation of Nb-rich intermetallic laves phase observed [18]. A higher solution annealing temperature will increase the Nb content in the super alloy as Nb is a major strengthening element and hence increase precipitation strengthening [19].

2.2.7. Coarsening of γ'' in Inconel 718

Gamma double prime phase constitutes Nb as the main strengthening element along with some extent of iron which provides the necessary electron to atom ratios and matrix to precipitate the required mismatch from gamma double prime. The coarsening of gamma double prime is followed by the formation of stable delta phase. To impede the coarsening of γ'', the (Al + Ti)/ Nb specific ratio comes into account. The controlled (Al + Ti)/ Nb ratio helps the γ'' to cover cuboidal γ' on all of its faces under certain thermal consideration [20]. On slow coarsening rate of gamma double prime the thermal stability of the phase improves. Then adjustment of (Al + Ti)/Nb ratio assist in lowering the coarsening rate of gamma double prime and formation of delta phase delayed [21]. According to some authors the study of thermal stability of INCONEL 718 has shown that rapid coarsening of the gamma double prime is caused by the over aging the specimen at above 750^0C [22].

2.2.8 Effect of Rhenium on coarsening kinetic of γ''

In modern days new super alloys are developing to increase the operating temperature and to achieve higher efficiency and lesser the emissions from the engines and other plants. To meet all this demands addition of Re was employed to Inconel 718 [23]. Rhenium is distributed selectively to the matrix phase and acts as a particular effective strengthener which retards the coarsening of γ''. It is stated that by the addition of 6% Re to the alloys the volume fraction of gamma increased by 0.83. Hence, the volume fraction of γ, and eutectic γ + Ni_2Nb phase variation is dependent on Re [24, 25]. With higher Re content larger the dendritic arm spacing. For the single crystal super alloys such as Inconel 718 the addition of Re up to 6% has been employed by various alloys designers [26, 28]. No major microstructural change can be observed in IN 718 by the addition of Re. The major change that is what Re is responsible for is the size variation of columnar or cellular dendrites in the gamma matrix. Re acts as a solid solution strengthener in Ni-based super alloys [27, 29]. As Re is not composed of carbides, there is no effect on the carbide precipitation due to change in Re. In gamma dendrites Re replaces Nb by forcing the Nb particles to the inter-dendritic regions where they can segregate into eutectic γ-NbC and γ-Ni_2Nb. With the increasing amount of Nb content in the inter-dendritic regions the volume fractions of carbide and Ni_2Nb increases [31].

2.2.9 Grain boundary phases

Delta phase mainly precipitates along the grain boundary at lower temperature. And at higher temperature carbide precipitation along grain boundary can be observed. Corresponding to γ'' phase δ phase is an equilibrium phase. Formation of this phase in Inconel 718 occurs at high temperature with long exposure [32]. Delta precipitation takes no part in strengthening but contributes in controlling the grains. It is non-coherent with the matrix and precipitates inter granularly at higher temperature and nucleates along austenitic grain boundaries at lower temperature [33]. At approx. 900^0C the fastest rate of delta formation can be observed. Precipitation starts at the grain boundaries of gamma phase through a reaction which is not continuous. Even at the presence of γ'' delta phase precipitates inter-granularly. It has been reported that in Inconel 718 the δ-precipitation causes a degradation to the mechanical properties. The reason behind this is the transformation of γ'' to δ in the microstructure [34, 20].

$$\gamma' \text{ (FCC)} \longrightarrow \gamma'' \text{ (BCT)} \longrightarrow \delta \text{ (Orthorhombic)}$$

Delta phase softens the material and reduces the strength of the material. The δ particles have needle like shape as well as plate like and processes blocky shape too. The needle like delta can be found nucleated at austenitic grain boundaries at above 650^0C or 750^0C [35, 25]. It is reported that blocky delta particle forms at a solution annealing temperature of 954°C and at around 800-900°C needle like delta formation is superior. To get the true morphology of delta phase deep etching is suggested. With increasing Nb content the formation of delta becomes more. Hence, it is stated that fraction of delta can be controlled by changing the Nb content. The structures of δ-Ni_3Nb and γ''-Ni_3Nb are crystallo graphically coherent but the basic difference lies on the stacking sequence of the planes. The volume fraction and as well as the precipitation kinetics are improved with increasing ageing temperature [36, 26].

2.2.10 Formation of laves phase

There are chances of formation of laves during heat treatment and during solidification both time. During solidification it can form inter- dendritically into the segregated regions. In most of the cases of super alloys at the end of the solidification process Nb rich intermetallic laves phase formation is usual [37, 34]. In both solid solution strengthening and precipitation hardening during solidification Nb tends to segregate in the inter-dendritic area. As high Nb

content (up to 22.4%) hampers the ductility of the super alloy, hence, this phase is a undesirable phase and harmful phase. This phase continues to remove alloying elements required for precipitation hardening and therefore it caused in reduction of strength [38]. The standard homogenization heat treatment temperature and exposure at which delta phase will completely dissolve and a portion of laves phase will dissolve is 1095°C for 1 hour. After heat treating for 15 minutes at 1050°C the presence of small and granular laves phase can be observed. On holding the specimen at 1095°C for 45 minutes the morphology of the phase does not change but the volume fraction decreases [39].

2.3 Heat treatment of INCONEL 718

It is confirmed by most of the authors that the ageing process of nickel based super alloy such as Inconel 718 is highly dependent on some material parameters. The nucleation process of different phases varies with temperature and exposure. It results in morphological changes in the precipitated phases. The mechanical properties such as strength, hardness, ductility, brittleness can also change according to the microstructural variation and another possible reason can be the effect of different heat treatment temperature. Examining the mechanical behavior of the material within the temperature range 500-750°C and microstructural changes in between that temperature is recommended by most of the authors [39-41].

2.3.1 Optimization of solution annealing temperature

For Inconel 718, before ageing it is essential to do solution annealing by making a solution of all the precipitated phases to make sure that the precipitation hardening will be advantageous. Some major constituents of Inconel 718 such as Fe, Ni and Cr, during solidification are partition to dendritic core and the other elements such as Ti and Nb find places to accumulate in the inter-dendritic portion. Such micro-segregation of elements and the phases which are not in equilibrium can cause variation in phase transformation and behavior during hardening. To eliminate this, solution annealing is performed [42]. Solution annealing before aging enhances the ductility and assist in grain growth. For nickel based super-alloys high temperature solution annealing is recommended to minimize the effect of hydrogen assisted cracking which takes place at lower temperature. In nickel based super alloys it has been found that when the solution annealing temperature is below 980°C there is no evidence of grain growth [43, 14]. To ensure about the exact grain growth temperature and about strength and ductility the Specimens were

undergone various solution annealing temperature in between the range of 850°C-1270°C [44, 35].

I. When the solution annealing performed at 850°C, it has been found that globular δ-Ni_3Nb particles were precipitated at particle boundaries.

II. At 955°C solution annealing temperature plate like delta along with globular morphology precipitates in the matrix and along grain boundaries.

III. The delta phase dissolved totally when the solution annealing performed at 1050°C as the δ solvus curve is reached.

IV. Solution annealing at 1095°C dissolves delta phase and a portion of laves phase. But still the presence of laves phase can be observed if slow cooling is performed after solution treatment at this temperature.

V. At 1150°C, all the primary carbides such as NbC, TiC or Nb and Ti rich carbides will dissolute and the volume fraction of the secondary phase particles will also decrease. At this temperature as the carbides are dis-solutes, excessive grain growth occurs.

VI. On further increasing the solution annealing temperature, such as at 1250°C, incipient melting occurs at the boundary regions of triple points.

VII. At 1270°C temperature, melting occurs at the particle boundaries which results in the disruption of the films of the boundary. It results in migration of the particle boundaries.

As no grain growth takes place at 980°C, soaking the alloy for 1 hour at that temperature will produce a solid solution which is highly homogeneous. Both gamma prime and gamma double prime phase nucleates in between 650°C to 900°C in very short period. Dissolution of the phases occur above this temperature. Needle like delta forms from gamma double prime twins and as well as from the gamma matrix in the range of 800-950°C [45, 35].

Compared to solution annealing at 980°C it has been reported that at 1095°C the grain growth takes place due to the disappearance of the grain boundary phase or delta phase which dissolves completely leaving behind the carbides in the matrix at this temperature [46]. High temperature solution treatment is recommended to obtain gamma matrix as an initial microstructural phase then followed by heat treatment at lower temperature than solution annealing temperature. The quenching process after solution treatment has a marked influence on the precipitation hardening. Water quenching, which is a rapid quenching process will enhance the ageing response and on the other hand air cooling or furnace cooling will tend to produce precipitation in the solution treated specimen.

2.3.2 Ageing cycles

To form gamma prime and gamma double prime both, it is necessary to do ageing treatment below solution annealing temperature. Because above 800°C these phase are no longer stable. Hence, the ageing cycles are performed mainly within 650°C - 900°C range.

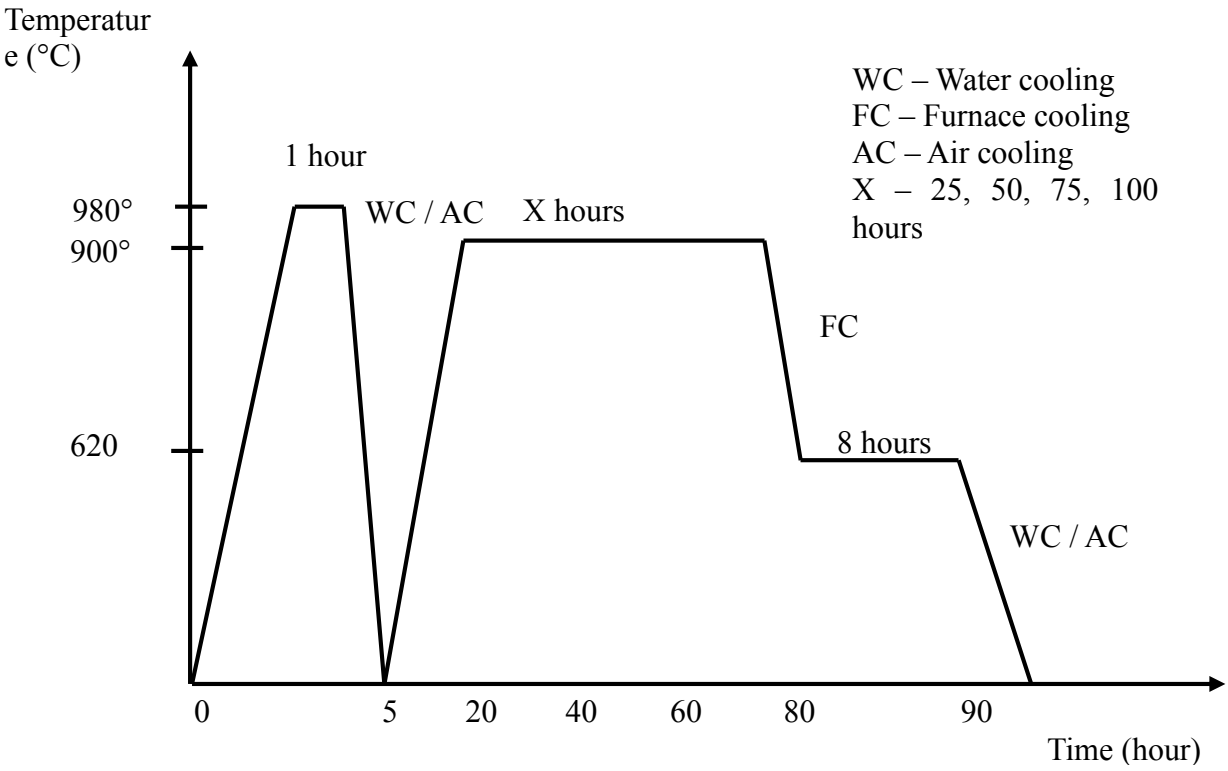

Fig 9. Heat treatment schedule at different temperature and exposure

For nickel based super alloys, the focus is to produce gamma prime in high volume fraction and improved size distribution which provides great stress rupture properties. In as cast Inconel 718 where the volume fraction of γ/γ' eutectic is sufficiently high, the importance is given to the dissolution of gamma prime. One of the major advantage of Ni-based alloys are high melting temperature which allows the gamma prime microstructure refinement with solution annealing followed by multiple stages of ageing [47]. A considerable number of heat treatment that is performed in intermediate stages is done to ensure about the variation in mechanical properties with the variation of microstructures. During ageing treatment the primary carbides breaks and follow the given reaction [48] –

$$MC + \gamma \longrightarrow M_{23}C_6 + \gamma'$$

The second stage heat treatment helps in increasing the size of gamma prime particles and enhances the formation of carbides at grain boundaries. But the gamma prime particles do not coalesce in this temperature. In the third step, secondary carbides such as NbC precipitates at the grain boundary at the cost of primary carbides and gamma matrix. The fourth stage heat treatment enhances the growth of metastable gamma double prime phase [49].

2.3.3 TTT diagram of Inconel 718

TTT diagram of solution annealed Inconel 718 is given below

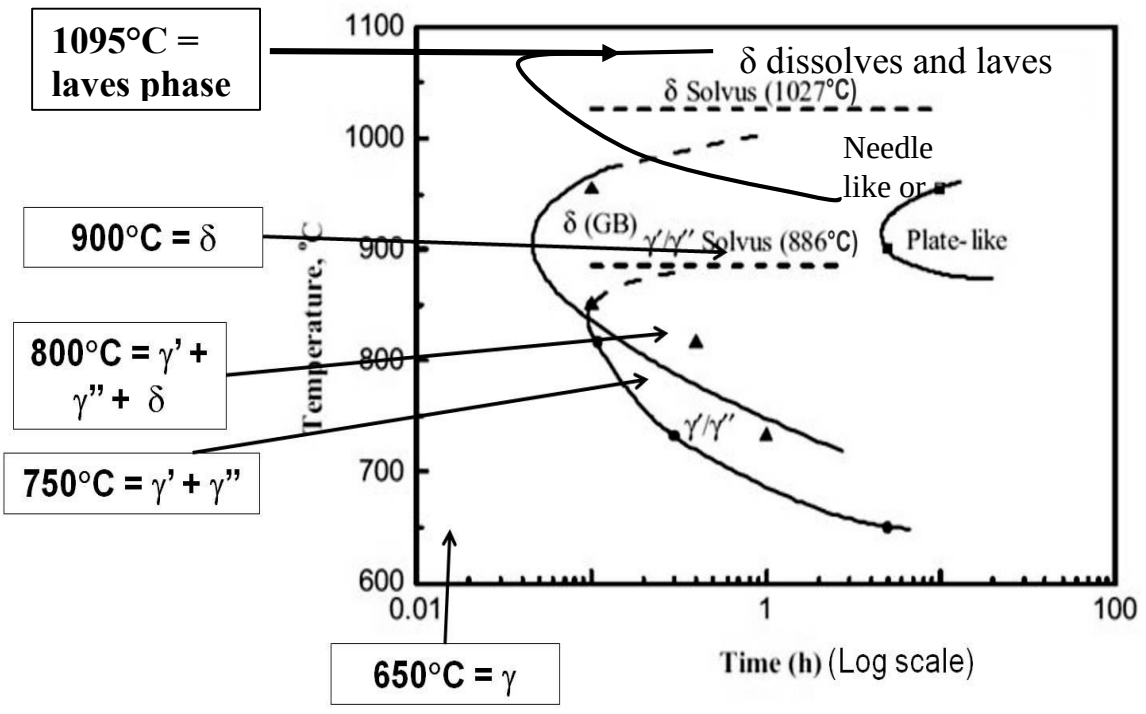

Fig 10. TTT diagram of Inconel 718

From the TTT diagram it is known that formation of gamma double prime starts at above 650°C and at 800°C delta formation takes place along with gamma prime and gamma double prime present in the matrix and at 900°C needle like or plate like delta forms. The ageing temperature employed for delta phase is very much close to the γ'' solvus temperature which is nearly about 900°C [48-49]. And there is no sign of laves phase formation in between 500°C - 1000°C. The type of precipitates and the beginning of precipitation depends on the characteristics of the starting material, i.e. the amount of delta particles left in the specimen after solution annealing. As the kinetic of nickel based super alloy is very slow, it is required long exposure at high temperature to expose the nature of the material. The precipitation of secondary phases are very slow which leads to take up to 50 hours to form gamma double prime [50].

2.3.2 Double ageing

The main purpose of double ageing is ensure about the enhancement of the formation of both gamma prime and gamma double prime. Keeping in consideration the industrial use of the alloy at 650°C and the instability of gamma prime and gamma double prime at above 800°C, among various kinds of double ageing technique the optimization was done performing the double ageing treatment at 720°C for 8 hours then furnace cooling then again at 620°C for 8 hours followed by water quenching. Such optimization was done considering the fact that this double aging treatment will produce higher contents of γ' and γ'' and it will form lower delta particles [51]. This treatment does not affect the grain size of the precipitates. The components prepared by double aging technique consist of homogeneous and fine grains, improved strength, good low cycle fatigue properties and capable of anti-crack extension. Double aging treatment assist the precipitation of delta particles along grain boundary in Inconel 718. Mostly stick shaped discontinuous delta formation takes place. Some of the discontinuous delta shifts from the grain boundary to inside the grains and nucleates there but the amount is very low. Distribution of disc shaped gamma prime and gamma double prime over the base matrix can be seen by the microstructural observation. [52, 38]. After the polishing and etching the SEM micrographs of double aged specimens reveals that inside grains, the spherical precipitates are gamma prime particles and the disc shaped particles are gamma double prime. After ageing at 720°C at the exposure of 8 hours it can be seen that the growth of both gamma prime and double prime are taking place but at 620°C the growth of gamma double prime stops and the gamma prime particles continues to grow [53]. The double ageing sequence is given in the below figure.

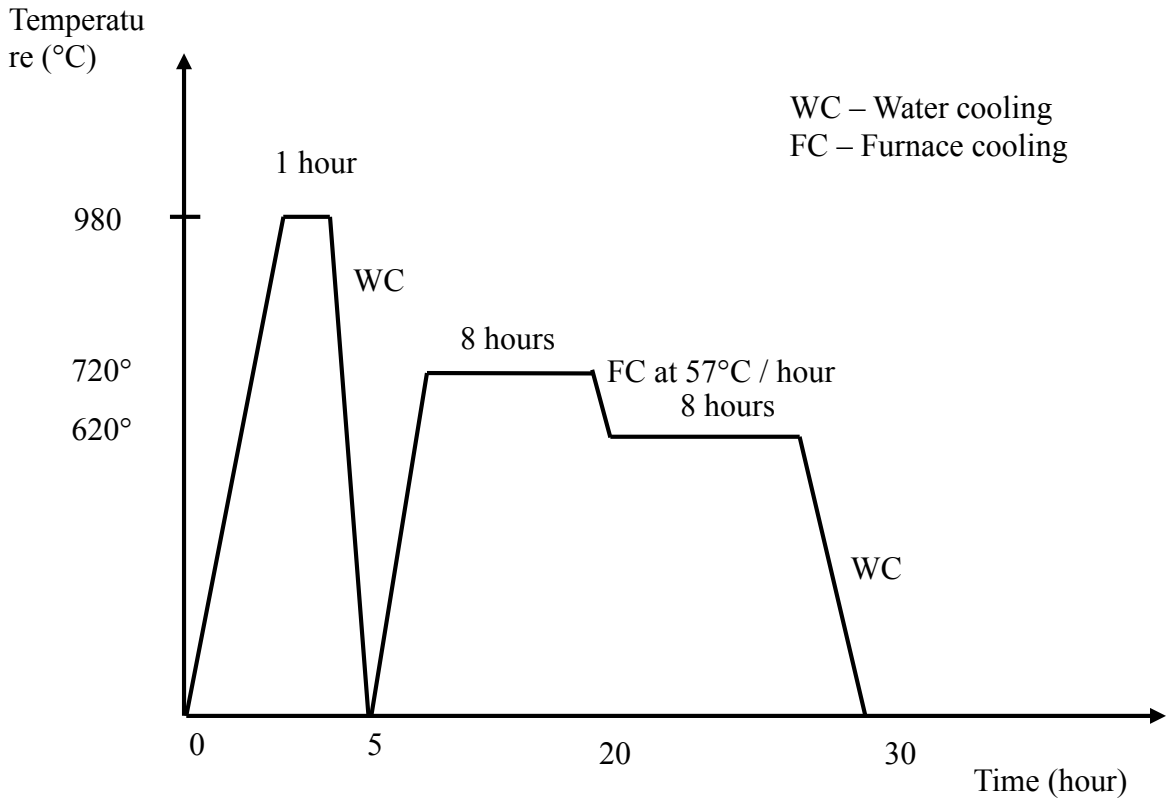

Fig 11. Double aging treatment schedule

After microstructural analysis of double aged specimen the resultant microstructures shows that about 14-15% fine gamma double prime particles which are fine and nano-sized are formed and thus enhances the strength of the alloy to an extent of 1400 Mpa. It is also revealed that few needle like delta and a considerable amount of carbides distributed over the matrix along with fine gamma prime and gamma double prime particles. By the EDS analysis it is get to known about the elemental composition of the carbide and the delta phase and formation of Ni or Nb composed precipitates [54].

2.4 Tensile properties of Inconel 718

For alloy 718 the study of room temperature and high temperature tensile tests results shows that at room temperature ductility is high but strength is low but at higher temperature ductility decreases comparatively and strength increases. Keeping in mind the structural stability of

Inconel 718 the tensile test temperature are optimized to 650°C because above this temperature the main strengthening phases such as gamma prime and γ´´ - Ni_3(Nb, Al, Ti) becomes instable and the gamma double prime changes into stable delta with increased size and plate like morphology [55, 39]. The specimen which were undergone tensile test at 650°C will possess high strength and lower ductility and it will vary with the ageing temperature. The change in ductility with the extended heat treatment temperature will cause decreasing Yield strength, Ultimate tensile strength and increasing elongation [56]. The solution treated specimen will possess comparatively lower yield strength but good ductility which is around 55% because all the strengthening phases dissolutes during solution annealing. When quenched in water the growth of matrix phase stops and it possesses lower strength due to the softness of the matrix. Another reason behind decreasing strength might be due to solution treatment reduction in dislocation density occurs and as well as internal stresses which helps in increasing ductility. The highest strength can be achieved at 750°C with a minor decrease in ductility which is due to the gamma double prime formation which leads to cut of the particles by dislocations. It will be possible to regain the ductility if we further heat treat the sample for shorter time and the temperature above the service temperature [57].

With the increasing ageing temperature the extent of decrement in UTS and YS increases and depends on the duration of ageing and as well as the dissolution of intermetallic precipitates. One of major strengthening phase Ni_3 [Al, Ti, Nb] had less influence on ductility but the yield strength is highly influenced by this. Delta phase which is comparatively softer that the strengthening phases is incoherent with the matrix phase and deleterious. The formation of delta occurs at higher temperature which results in decreasing the yield strength, ultimate tensile strength and increased elongation [58]. At the highest temperature, the maximum load occurs which may be not due to the necking but from the over-ageing of the precipitation hardened microstructural phases. At high temperature the test is dependent on strain rate also. Higher the temperature of test, with the increase of strain rate the strength properties are also increased while at all temperature the uniformity in elongation of the specimen tends to increase with increasing strain rate. The optimized strain rate for performing tensile tests at 650°C is 10^{-3}mm/sec [59].

Chapter 3. EXPERIMENTAL

3.1 Material and preparation of specimens

From a forged Inconel 718 cylindrical bar of length 75mm and diameter 160mm, different specimens were cut using EDM wire cut for our experimental work. The sample dimensions are as follows-

I. 12 blocks of dimension 15mm × 15mm × 10mm with parallel opposite face for microstructural studies.
II. 20 Tensile specimen (circular cross section with thread in both ends) of diameter 6mm and gauge length of 15mm as per ASTM standard E 8M.

All the samples were heat treated accordingly in a controlled way using a Carbolite furnace which can be operated up to a maximum temperature of 1400^0C.

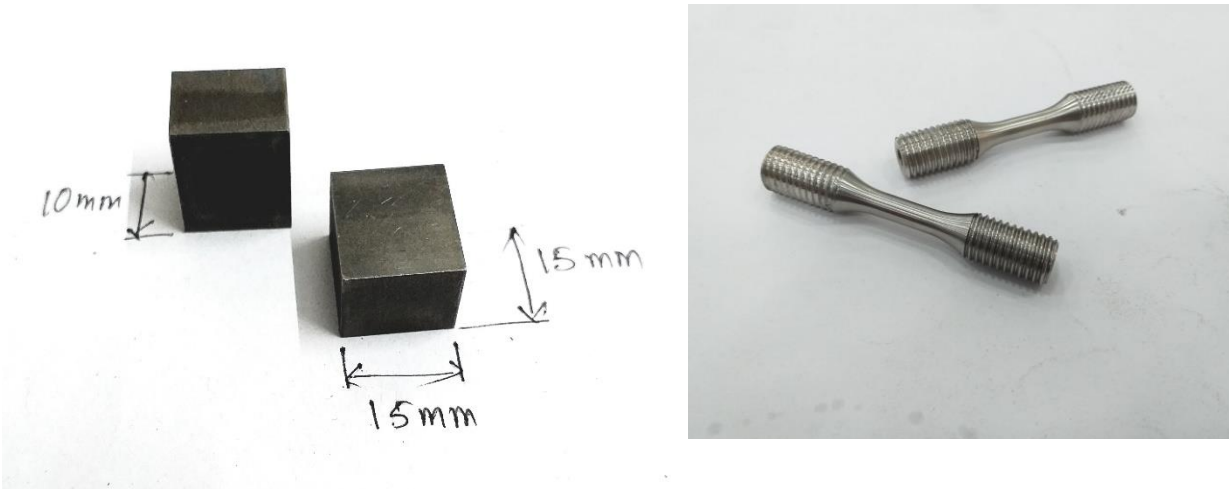

Fig 12. Specimens prepared for microstructural analysis and tensile tests

3.2 Heat treatment schedule

The heat treatment operations through which the block and tensile samples were undergone is described as follows-

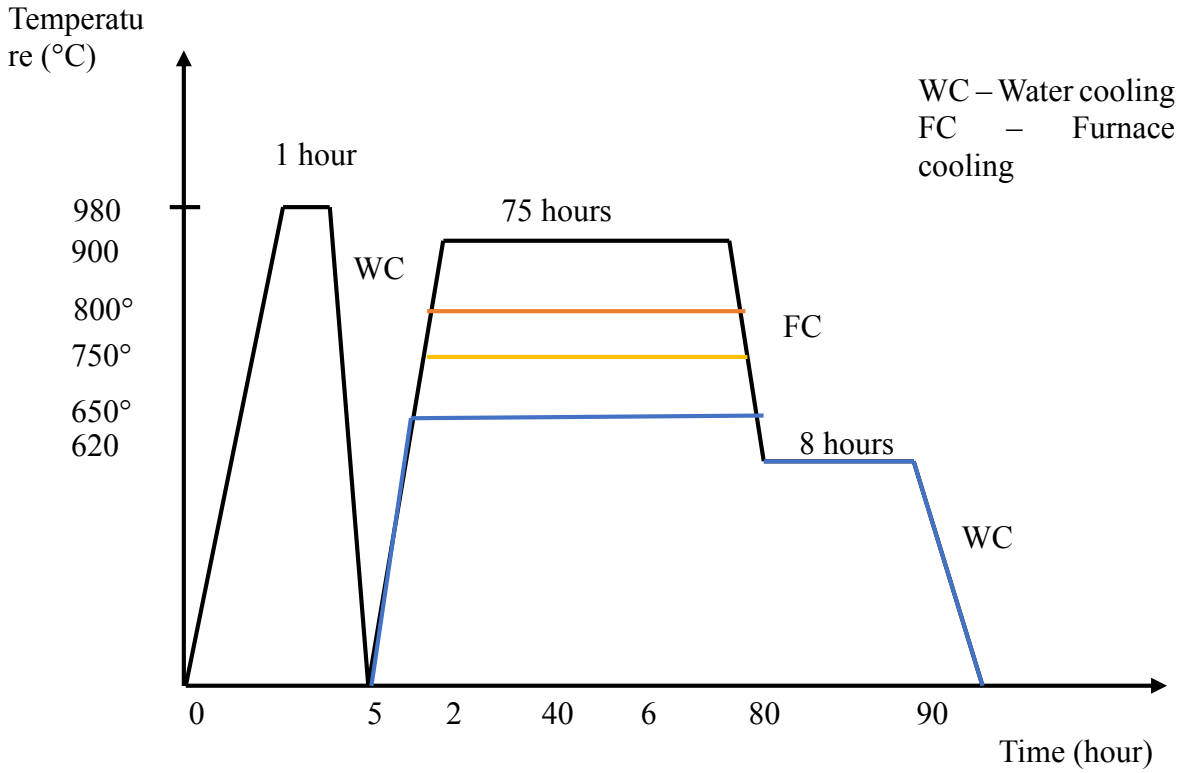

Fig 13. Heat treatment schedule for four specimens at four different temperature

After solution annealing the samples were went through further ageing treatment in two steps. At first step, was at the exposure of 75 hours and in 2nd step the exposure was 8 hours. As the kinetic of this super alloy is very slow, the samples were allowed to go through long exposure to reveal various microstructural phases. A variety of heat treatments were performed to obtain desired phases such as gamma (γ), gamma prime (γ'), gamma double prime (γ''), delta (δ) and laves phase by precipitation phenomenon. The following table shows with varying heat treatment temperature and exposure the expected phases to be obtained.

Table 1. Expected phases with different temperature and exposure

Solution annealed at 980°C for 1 hour	Solution annealing + heat treating at 650°C for 75 hours	Solution annealing + heat treating at 750°C for 75 hours	Solution annealing + heat treating at 800°C for 75 hours	Solution annealing + heat treating at 900°C for 75 hours
Gamma (γ)	Gamma (γ) + Gamma prime (γ′)	Gamma prime (γ′) + Gamma double prime (γ′′)	Gamma prime (γ′) + Gamma double prime (γ′′) + Delta (δ)	Delta (δ)

After thermal ageing of all the samples including blocks and tensile specimens, those are removed from the furnace and quickly quenched in water for rapid cooling to stop the growth of precipitates further. Then the sample were kept preserved in envelopes separately for our further use.

3.3 Metallography

After heat treatment the sample surfaces became rough. Hence mechanical polishing was required to proceed further for phase evaluation. All the blocks were taken and mounted for the ease of holding. Copper powder was used as mounting material. Then mechanical polishing was done in two steps both paper polishing and cloth polishing. For paper polishing Silicon carbide papers were used from grade 80 up to 2500 for fine polishing. The cloth polishing was performed using diamond solution for some time up to a certain level of fineness then checked in optical microscope in regular interval to observe if there is any scratches or pits on the surface of the sample. After finishing cloth polishing the samples were cleaned using soap or hand-wash then dried and kept preserved for etching. The etchant used for this purpose was a mixture of aqua regia and glycerol. Amounts of the constituents were varied accordingly considering light etching and deep etching wherever required. Aqua regia is a good etchant for Ni-based super alloys to reveal the microstructure. Some amount of glycerol was mixed with it as aqua regia is a strong acidic solution and it can cause over etching of the sample surface. Glycerol lowers the etching rate.

After etching the samples were cleaned by methanol. To observe the microstructure a HITACHI S-3400N Scanning Electron Microscope was used. SEM micrographs of various heat treated specimen's surface were captured up to 3000X magnification and EDS has also been taken to get compositions of the precipitates formed.

3.4 Vicker's macro Hardness test

After microscopy the samples were undergone vicker's macro hardness test. The aim was to correlate the change in hardness with different heat treatment effect. The testing was done using Econamet VH-50MD hardness testing machine which can be operated up to a load of 50 kg-f. The method was to indent the sample surface with a diamond indenter applying 30 kg-f load and then measuring the indentation diameter. For each sample this process was repeated for 5-6 times in different locations to take the average value. Another important factor that should be taken into account is the indentation time. For our sample surfaces we used 10s indentation time for each indentation. The diamond indenter when hits the surface it lefts an indentation

mark there. By the use of eyepiece and lens and given scale there the length of the two diagonals of the indentation D_1 and D_2 is measured. The hardness display on the screen as HV_X where X stands for the value of hardness.

3.5 Room temperature and high temperature Tensile test

Tensile tests were done both in room temperature and high temperature to get the variation of yield strength and ultimate tensile strength with different heat treated condition and different testing condition. For each sample repeated tests were also done (high temperature only). The tensile specimens were made according to the ASTM standard E 8M. Each sample was of circular cross section and threaded in both ends. The tensile specimens were also heat treated according to the schedule and exposure. At first one test was performed on the as received sample without solution annealing or any other heat treatment to use this as a reference so that the improvement or degradation of other test results can be compared with this result. As per the sample geometry two M12 step nuts were used to hold the sample with the fixture. For room temperature tensile test a 2620-601 dynamic extensometer of gauge length 12.5 mm was used. It can travel 40% that means can elongate its arms up to 5 mm. For high temperature tensile test a 3549-0050-100-ST axial furnace extensometer of 12.5 mm gauge length and which can withstand up to 1200^0C (2200^0F) with 100% travel was used. The high temperature tensile tests were performed at 650^0C because INCONEL 718 is not used above 650^0C for industrial work purpose. Above that temperature instability of main strengthening phases will arise due to formation of stable weaker phases and the alloy will lose its structural stability.

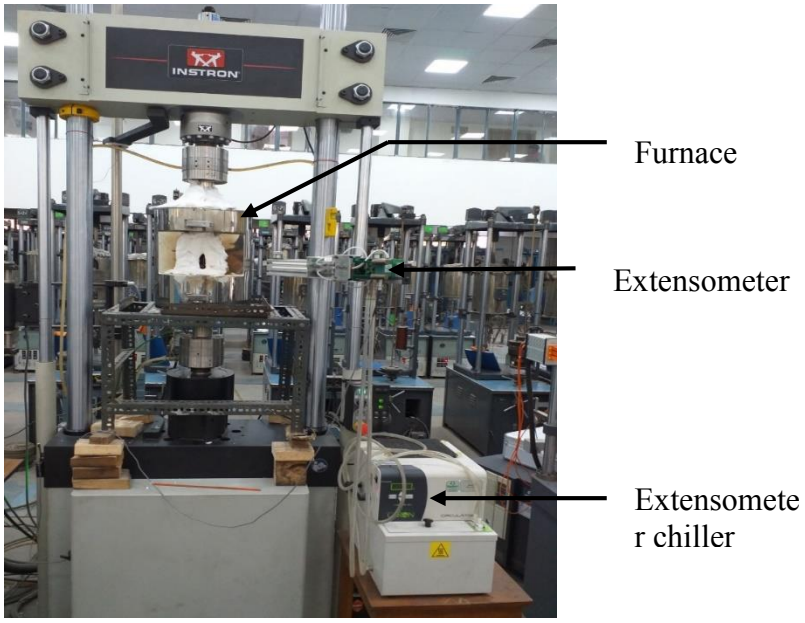

Fig 14. Servo electric INSTRON 8862

The room temperature tensile test was carried on using a servo hydraulic INSTRON 8501 which has a capacity of 50 kN. And the high temperature tensile tests were performed in a servo electric INSTRON 8862 of 100 KN capacity. The temperature was raised by a furnace attached by thermocouples which can be operated up to 1100^0C. High temperature lubricant was used in the threads of the pull rod and threads of the samples so that during heating due to thermal expansion the threads of both pull rod and sample do not interfere with each other and do not tighten while cooling and to protect the threads from high temperature oxidation. To prevent the heat loss from the furnace to the surroundings during test glass wool was used to cover the furnace exposures. As the pull rods are continuously exposed at high temperature during test, for cooling system continuous supply of chilled water through pipes was given. When test temperature reached, for 15-20 minutes the test specimen was soaked then the high temperature extensometer was inserted within the furnace and attached with the sample. By the use of a chiller the extensometer kept cool during the entire test. The room temperature tensile test input data is given in below table-

Table 2 – Room temperature tensile test inputs

Specimen name	Test code	Average gauge diameter	Gauge length	Strain rate	DAQ (Data acquisition rate)
IN_1	IN_1RT	6.03	13.49	0.001	0.002
IN_2	IN_2RT	6.03	14.80	0.001	0.002
IN_3	IN_3RT	6.033	13.22	0.001	0.002
IN_4	IN_4RT	5.973	12.90	0.001	0.002
IN_S	IN_SRT	6.01	13.84	0.001	0.002

The high temperature tensile tests input data which were carried out at 650°C is provided in below table-

Table 3 – High temperature tensile test inputs

Specimen name	Test temperature	Test code	Average gauge diameter	Gauge length	Strain rate	DAQ (Data acquisition rate)
IN_1	650°C	IN_1HT	6.07	13.28	0.001	0.002
IN_2	650°C	IN_2HT	6.03	13.64	0.001	0.002
IN_3	650°C	IN_3HT	6.04	13.87	0.001	0.002
IN_4	650°C	IN_4HT	6.02	14.06	0.001	0.002
IN_S	650°C	$IN_{S1}HT$	5.95	13.84	0.001	0.002
IN_S	650°C	$IN_{S2}HT$	6.03	13.96	0.001	0.002
IN_S	650°C	$IN_{S3}HT$	5.89	13.76	0.001	0.002

3.6 Fractography

After tensile test, to study the fracture surfaces of the specimens fractography was done. For this purpose from one of the two fractured parts from each specimen was taken and by the use of abrasive cutoff machine they were cut into equal pieces along the cross section from a distance of 8-10 mm from the fracture surface. While cutting precaution should be taken so that the fracture surface left unharmed.

3.6.1 Ultrasonic cleaning

After cutting into pieces the fractured samples required ultrasonic cleaning to remove dirt, pits from the surface before taking them to SEM for fractography analysis. Acetone was used as cleaning agent. The samples were hold for 5 minutes in a beaker which was subjected to ultrasonic velocity in a S 30H Elmasonic ultrasonic cleaning machine.

Chapter 4. Result and discussion

4.1 Evaluation of microstructure

4.1.1 Specimen IN_0

From the SEM images of etched block specimens which were heat treated in different temperature and exposure the presence of our desired phases such as gamma, gamma prime, gamma double prime and delta is found. Following figure shows the SEM micrographs of a sample solution annealed at 980^0C for 1 hour and then water quenched.

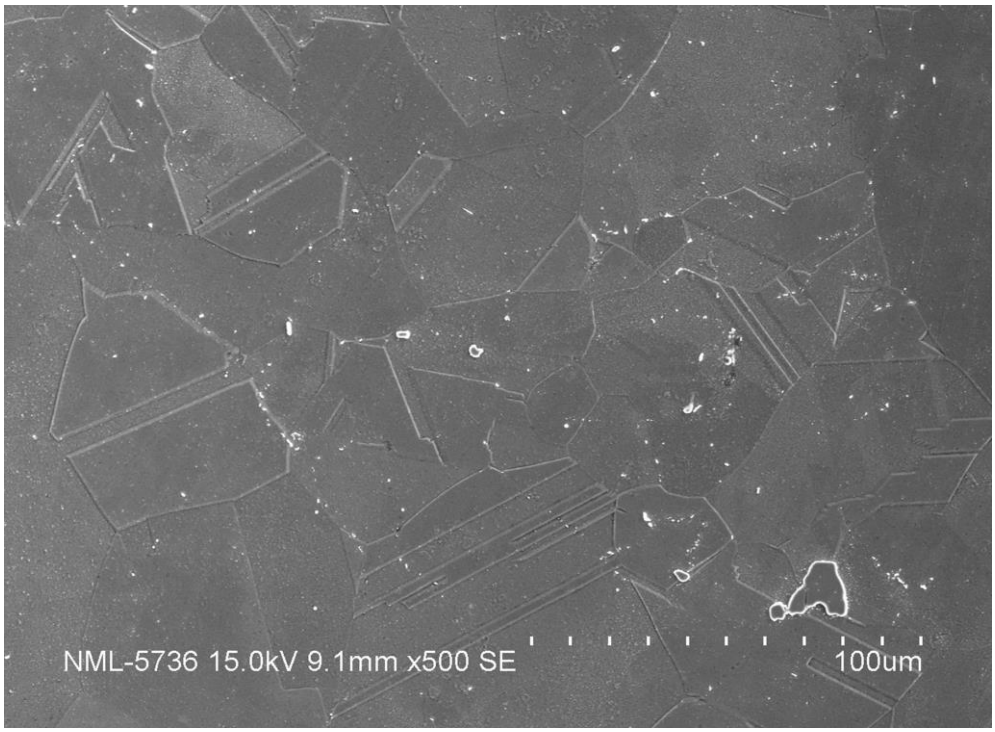

Fig 15. Sample solution annealed at 980^0C for 1 hours then water quenched shows the gamma matrix phase where all the phases are dissolved.

It is seen from the micrograph that solution annealing at 980^0C for 1 hour causes dissolution of all precipitated phases in the gamma matrix phase which is homogeneously distributed over entire area. As rapid cooling was done, it enhanced the ageing response and there is no sign of laves phase formation but carbide precipitates has formed in some regions. Slow cooling might have produced excessive delta and laves precipitation which contains high amount Nb as major constituent. There are some precipitates formed along grain boundary and inter-granularly over

the gamma matrix. From the EDS data given below the composition of the precipitates are found.

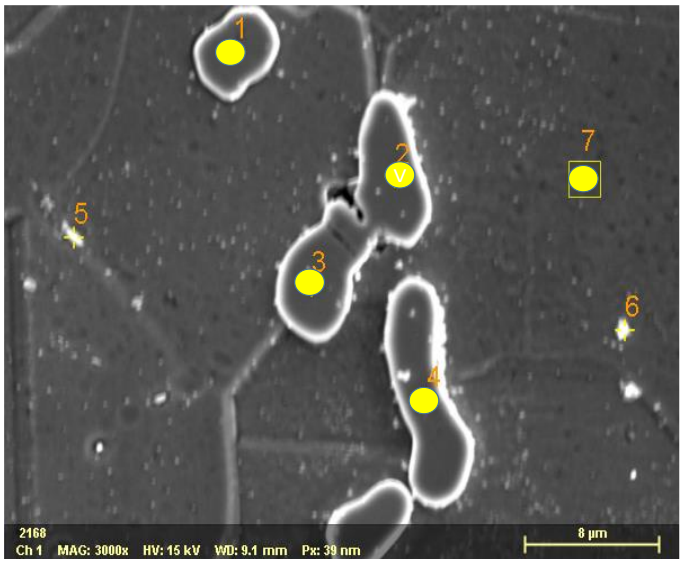

Fig 16. SEM micrograph of IN_0 taken at 3000X for EDS analysis.

The data from the x-ray spectrums are given in below table-

Table 4 – EDS data of block IN_0

Spectrum	C	O	Ti	Cr	Fe	Ni	Nb	Mo
1	15.88	1.60	5.12	0.12	0.29	1.06	74.62	1.32
2	17.19	0.25	6.00	0.46	0.16	1.09	73.16	1.69
3	16.07	1.31	6.78	0.28	0.13	1.40	73.03	1.00
4	15.72	0.09	5.99	0.42	0.05	1.03	75.30	1.38
5	14.64	1.47	1.48	15.97	9.37	21.68	18.77	16.61
6	6.76	0.70	1.06	18.07	15.48	38.16	12.09	7.67
7	5.60	0.47	1.05	18.93	17.95	46.96	5.80	3.24

In the above fig. there are some precipitates distributed over the matrix. The EDS data revealed that these precipitates contains Nb in high wt% and a moderate wt% of carbon so it can be said that Niobium carbide formation took place along the grain boundary as well as over the grains.

4.1.2 Specimen IN_2

After solution annealing of all the block specimens they were undergone several heat treatment operations. The samples were heat treated at different temperature and exposure. The following

figure shows the SEM images of a solution annealed specimen heat treated at 750^0C for 75 hours and then at 620^0C for 8 hours. Expected phase at this temperature is gamma prime and gamma double prime.

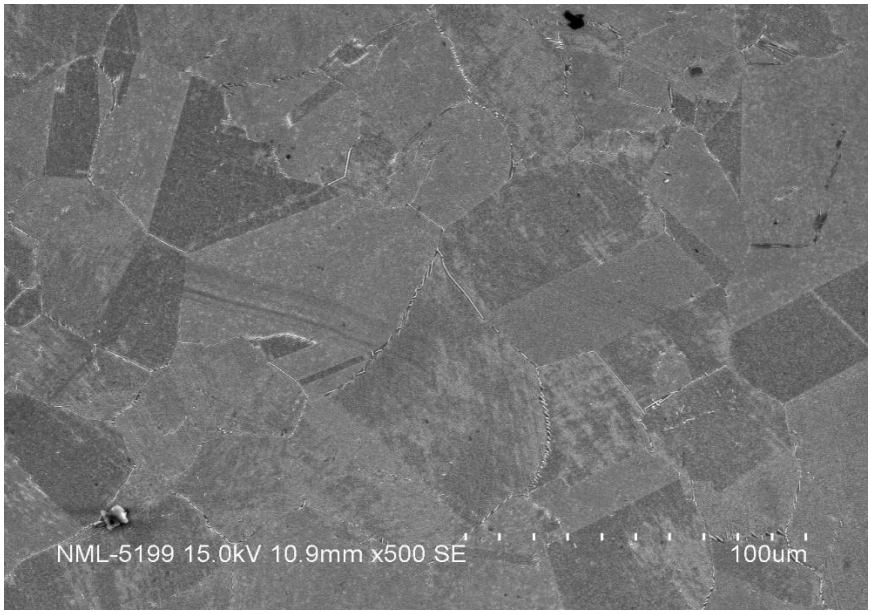

Fig17. Specimen solution annealed then heat treated at 750^0C for 75 hours then soaked at 620^0C for 8 hours followed by water quenching shows the precipitation of intermetallic phases along grain boundary.

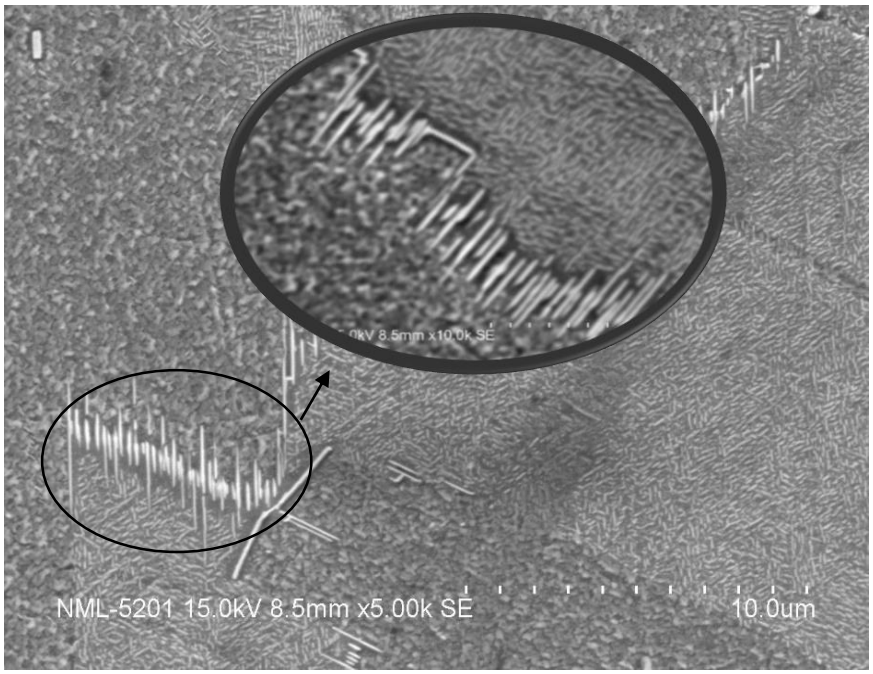

Fig 18. Nucleation of grain boundary phases starts slowly at 750°C

It is clearly seen from the SEM micrograph that for the sample heat treated at 750°C for 75 hours that intermetallic phases precipitated extensively. A closer observation (at 5000X magnification) will reveal that the intermetallic that formed in the matrix is the (γ′ + γ′′) intermetallic phase. From the above fig. it is also seen that the easy nucleation of the secondary phase is slowly taking place over the gamma matrix. In below fig. the photo was took at higher magnification to get a look over the precipitation of intermetallic phases. The EDS analysis of the sample is given below-

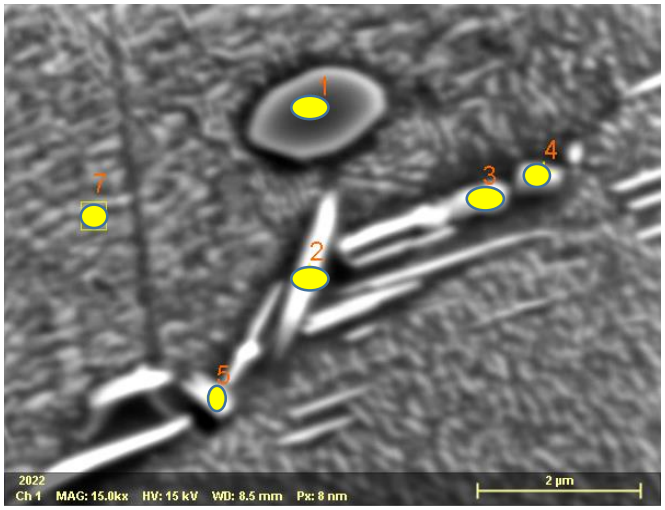

Fig 19. SEM micrograph of IN_2 taken at 15000X for EDS analysis

The data from x-ray spectrums are given in below table-

Table 5 – EDS data of block IN_2

Spectrum	C	Al	Ti	Cr	Fe	Ni	Nb	Mo
1	18.58	0.11	6.19	5.13	4.28	9.19	52.75	3.78
2	7.65	0.00	0.85	17.40	16.95	46.93	6.07	4.15
3	6.26	0.52	1.11	16.23	16.07	48.09	8.02	3.70
4	8.08	0.42	0.97	16.01	17.08	48.16	5.97	3.31
5	7.19	0.57	0.91	17.69	18.95	47.34	3.82	3.54
6	9.14	0.51	0.97	17.23	16.84	46.22	5.54	3.54

It is seen from the above SEM micrograph (fig.) that there are some precipitates over the matrix. By the EDS analysis it is seen that in region 1 amount of Nb is high and it formed niobium carbide but in region 2 amount of carbon is slightly more than the previous, so carbide

formation in this region took place enormously. We can distinguish them visually, region 2 is whitish totally and it indicates the region with high carbide content and region 1 is slightly blackish white and it indicates the region with comparatively less carbide content and Niobium rich. So, from the SEM micrograph of the sample heat treated at 750^0C it can be concluded that with increasing the heat treatment temperature and with long exposure the primary strengthening phase gamma prime and secondary strengthening phase gamma double prime both are present in the sample.

4.1.3 Specimen IN_3

After studying the morphology of the phases at 750^0C when the heat treatment temperature increased to 800^0C for another specimen for 75 hours and then again furnace cooled up to 620^0C then soaked the sample for 8 hours followed by water quenching, the SEM images revealed that delta phase nucleates along the grain boundary and as well as inter-granularly at the expense of gamma double prime.

Fig 20. Sample solution annealed then heat treated at 800^0C for 75 hours and then soaked at 620^0C for 8 hour followed by water quenching shows that needle shaped delta formed and gamma double prime has coarsen.

Though Nickel based alloys are mainly strengthened by gamma double prime (γ''), when it is aged above 650^0C the over ageing caused the formation of delta (δ) phase as gamma double prime is a metastable phase. At 800^0C rapid coarsening of γ'' causes the formation of delta in high rate.

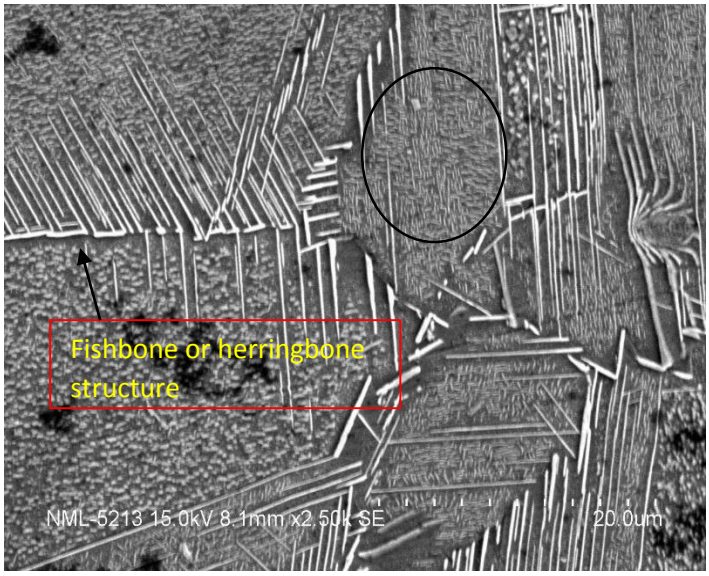

From the given fig. it is clearly seen that needle like delta formed along grain boundary which is looking like fishbone structure or herringbone type. Coarsening of plate like metastable gamma double prime can also be seen as the growth of δ phase increased compared with the specimen heat treated at 750^0C.

Fig 21. Clear view of nucleation of delta needles along grain boundaries

The following fig. indicates the enlarged section which was taken at 10000X magnification of a region of the above fig. In this figure the presence of plate like gamma double prime precipitates can be observed. And at 800^0C, the non-homogeneity of this phase is observed as coarsening kinetic of γ'' is high at this temperature.

Apart from the needle shaped delta there are some other precipitates which are having rod like shape. As the tips are blunt so it is not a needle like shape and not delta precipitate as well. So, presence of other precipitates are also observed there. The compositions of the precipitates are found by the EDS analysis which is given below. From the EDS analysis it is found that in region 1 gamma double prime particles are distributed and in region 2 and 3 delta formation started. It occurs due to high Nb content in that area (above 5%) and low (Al + Ti) / Nb ratio. From the above EDS data it has been found that in region 3 where (Al +Ti) / Nb ratio is 0.203 which is very low, delta formation has taken place in that region at the expense of gamma double prime.

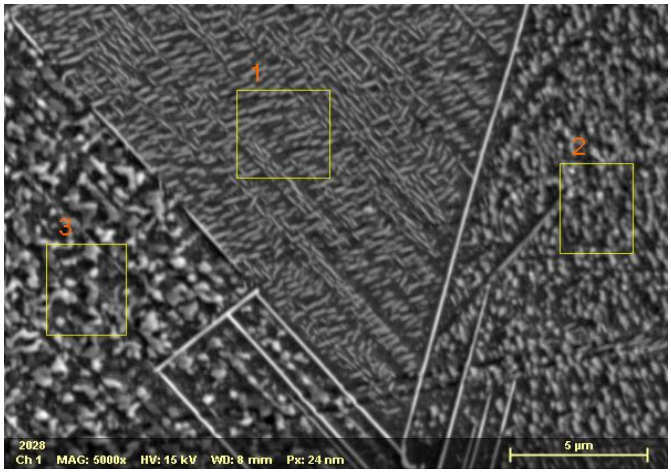

Fig 22. SEM micrograph of IN_3 taken at 5000X for EDS

The EDS data from the x-ray spectrum is given the below table-

Table 6. EDS data of block IN_3

Spectrum	C	Al	Ti	Cr	Fe	Ni	Nb	Mo
1	12.20	0.61	1.19	16.94	16.59	43.97	4.96	3.54
2	11.96	0.34	1.08	16.62	17.51	44.74	4.85	2.91
3	11.33	0.45	0.66	16.08	16.54	46.02	5.33	3.59

As the (Al + Ti) content start increasing which is 1.80 in region 1, the plate like precipitation starts forming which is gamma double prime.

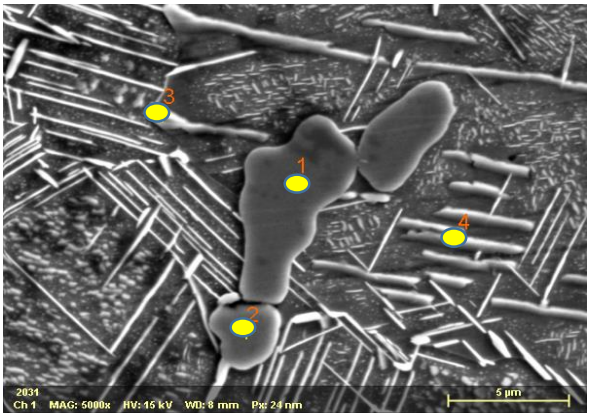

Fig 23. SEM micrograph of sample IN_3 taken at 5000X to get a closer view of carbide precipitation and the presence of delta phase and EDS analysis

From the above SEM image and the EDS data given in below table it is clearly seen that the apart from the delta needles there are Nb rich precipitates which is indicated by 1 and 2 where the precipitates contains high amount of Nb (66%) and formed Niobium Carbide as carbon % is also high in those regions.

Table 7 – EDS data of block IN_3 (carbide formation)

spectrum	C	Al	Ti	Cr	Fe	Ni	Nb	Mo
1	22.66	0.18	4.22	0.33	0.36	0.87	66.62	4.76
2	22.87	0.11	3.49	0.51	0.08	1.15	66.21	5.58
3	18.31	0.17	1.64	8.15	8.01	42.65	17.32	3.74
4	19.05	0.16	1.17	12.38	12.26	40.69	10.48	3.81

4.1.4 Specimen IN_4

Fig 24. Specimen solution annealed then heat treated at 900°C for 75 hours followed by water quenching shows that the secondary intermetallic phases are all dissolved and rapid growth of needle like delta formation.

With further increment of ageing temperature the complete growth of needle like δ phase can be observed. Another specimen which was undergone a heat treatment operation at a temperature of 900^0C for 75 hours has shown the above morphology. It is clearly seen from the above image that the growth of delta needles has taken place all over the area. The secondary phases such as γ' and γ'' has completely dissolved at this temperature and the

prolonged exposure helped in the transformation of γ'' to delta. Unlike the delta formation at 750^0C along grain boundaries, in this case we have found that the precipitation of δ phase took place inter-granularly as well as in grain boundary. So , it can concluded from here that at lower temperature delta phase nucleation occurs at austenitic grain boundaries but at higher temperature it precipitates inter-granularly as well. The EDS analysis of the above marked area 1,2 and 3 revealed that the region 1 and 2 is highly Nb rich area with almost 72% wt% of Nb and this is grain boundary region. So, it can be said that carbide precipitation took place in grain boundary region.

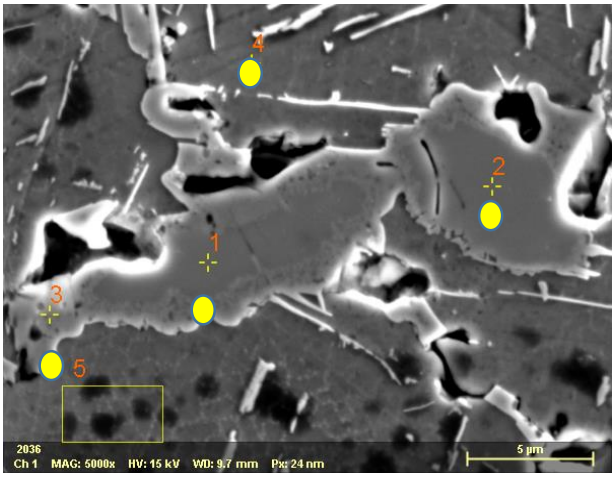

Fig 25. SEM micrograph of IN_4 taken at 5000X for EDS

Table 8 – EDS data of block IN_4

spectrum	C	Al	Ti	Cr	Fe	Ni	Nb	Mo
1	14.11	0.03	6.61	0.27	0.11	1.33	70.81	6.73
2	14.33	0.12	5.06	0.22	0.34	1.09	72.62	6.21
3	7.92	0.54	0.15	1.18	2.70	53.45	29.52	4.55
4	7.16	0.14	0.65	12.68	20.84	51.09	3.90	3.55
5	5.98	0.07	0.30	12.64	21.44	53.23	2.69	3.65

From the above analysis it can be concluded that at lower temperature precipitation of delta takes place slowly but at higher temperature about 900^0C the precipitation rate of delta is faster and it is dependent on Nb content.

4.1.5 Specimen IN_1

The below micrograph represents another heat treated sample surface which was carried out at 650^0C for 75 hours then soaked at 620^0C for 8 hours has shown coherency with the matrix gamma as the twin boundaries are visible here as well. From the SEM micrographs of this specimen it is clearly seen that the sample will remain in the gamma phase as there is no morphological changes in the microstructure observed. At this temperature carbide precipitation did not take place and the grain boundaries are visible clearly.

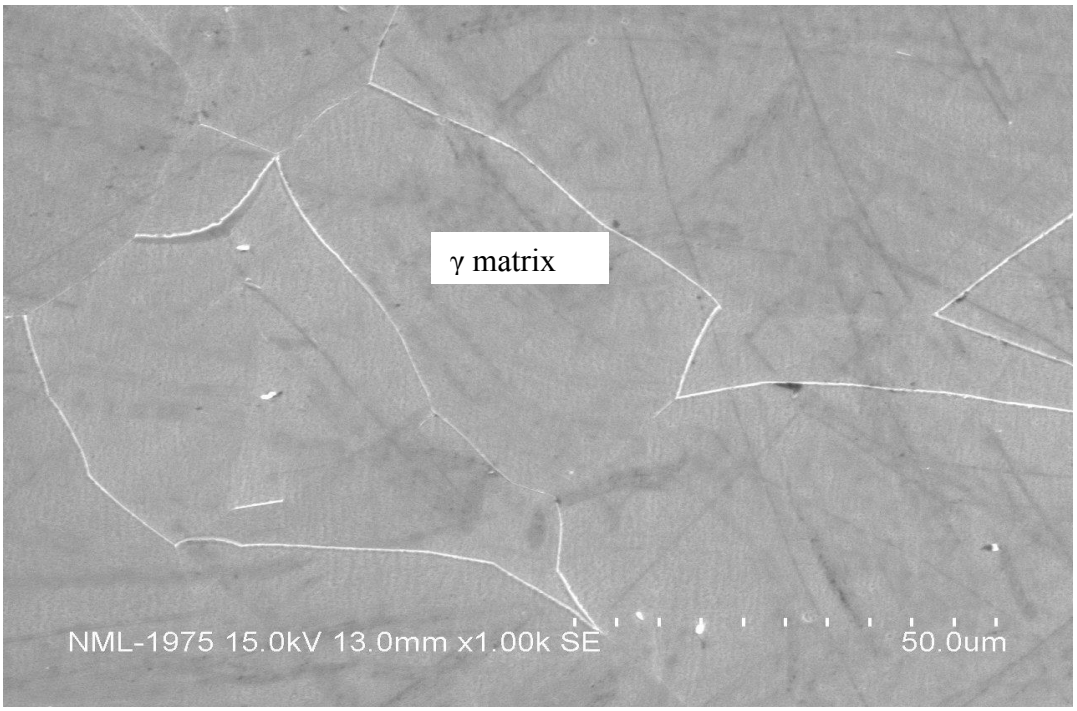

Fig 26. Sample solution annealed then heat treated at 650°C for 75 hours and then soaked at 620°C for 8 hours shows that existence of matrix phase along with intermetallic precipitation along grain boundary.

4.1.6 Specimen IN_{AR}

The as received Inconel 718 specimen has shown the below described morphology. Smaller grains are visible compared with heat treated specimens and some precipitates are shown over the surface that might come during solidification. The below given figure indicates the SEM micrograph taken at 500X magnification of as received specimen after polishing the surface and etching with aqua-regia solution and glycerol to reveal the microstructure.

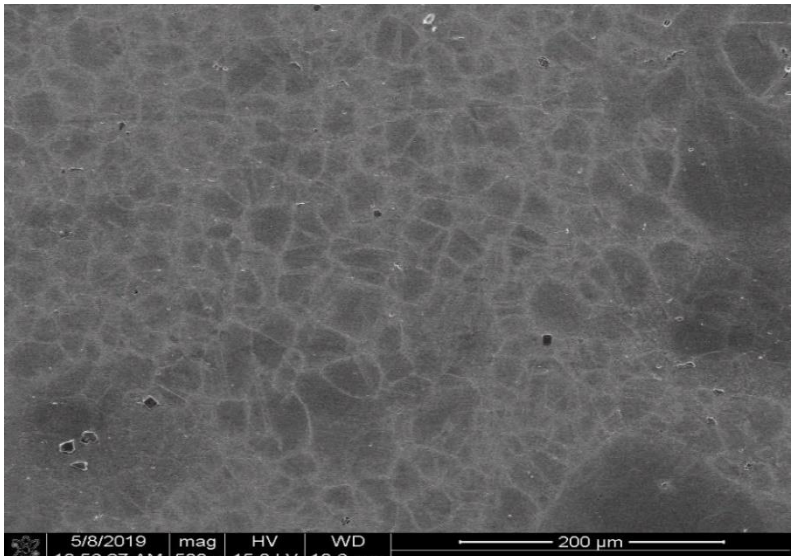

Fig 27. SEM micrograph of as received sample shows smaller grains randomly distributed

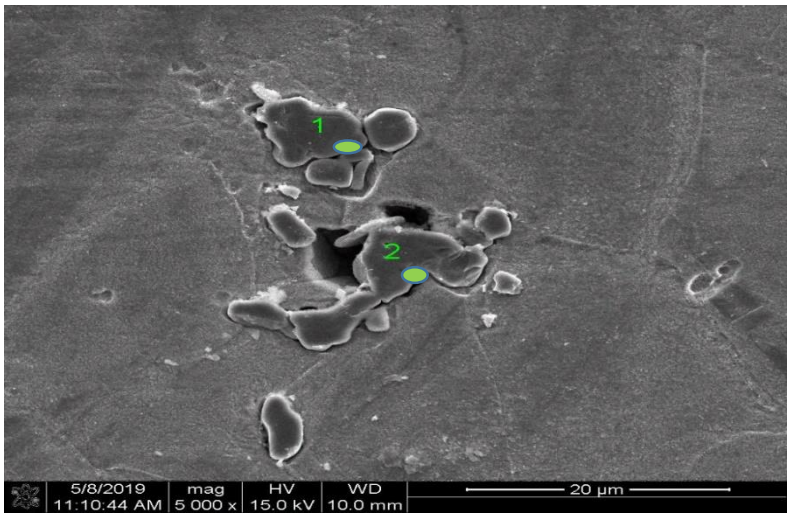

Fig 28. SEM micrograph of as received sample taken at 5000X for

From the EDS analysis of the above micrograph it has been found that the marked region 1 and 2 are highly Niobium rich and from some places carbide precipitates got removed during polishing. The data received by the x-ray spectrums during EDS is tabulated below.

Table 9 – EDS data of as received block specimen

spectrum	C	Nb	Mo	Ti	Cr	Fe	Ni
1	12.82	69.26	2.74	4.74	1.46	2.31	2.26
2	15.62	68.05	4.12	3.54	1.52	2.11	2.86

4.1.7 Specimen INs

The SEM micrograph of standard heat treated specimen is given below.

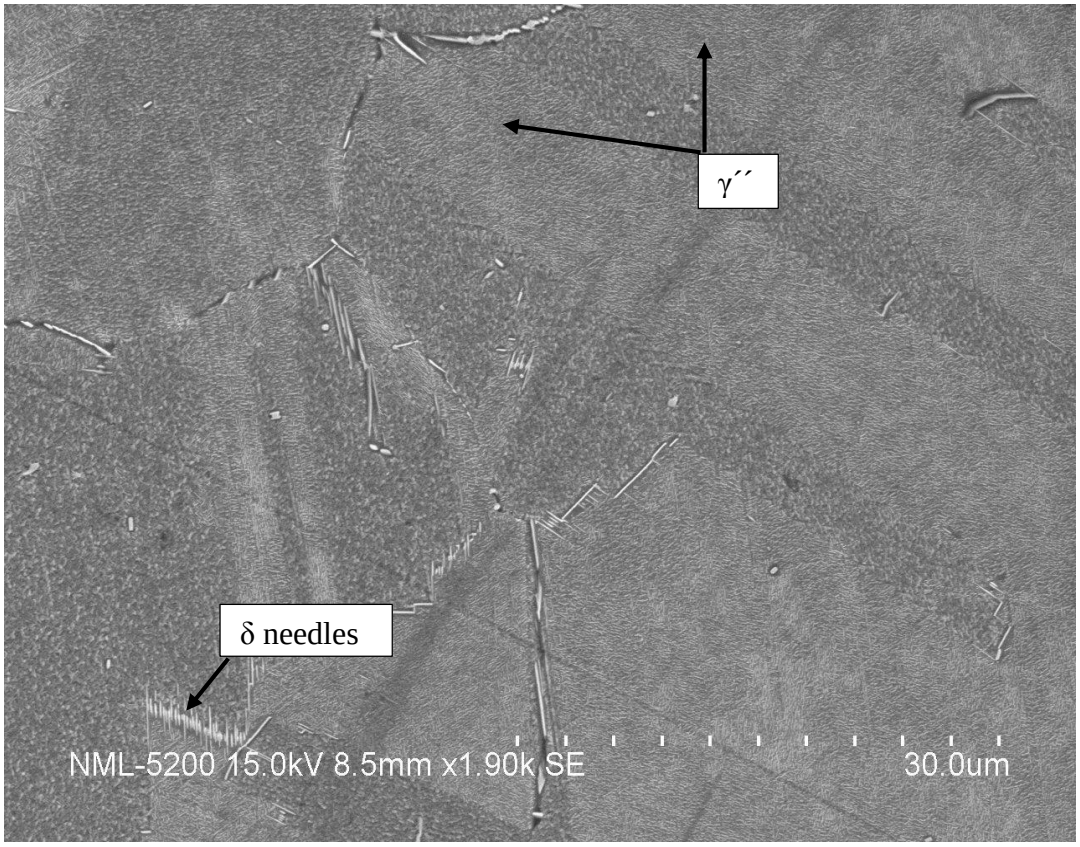

Fig 29. Specimen undergone double ageing treatment shows fine gamma double prime particles distributed over the area and in some particular region at the grain boundary delta nucleation just started

The standard heat treated specimens after microstructural analysis, it is found that there are uniform distribution of major strengthening phase gamma double prime over the matrix which is a stable phase at this temperature. There is no major sign of grain boundary phases but at some regions in grain boundary needle like delta nucleation just started. The standard heat treated specimen possesses highest strength due to the stability of main strengthening phase at this temperature. To get the compositions of the microstructural constituents EDS analysis was done which is given in below.

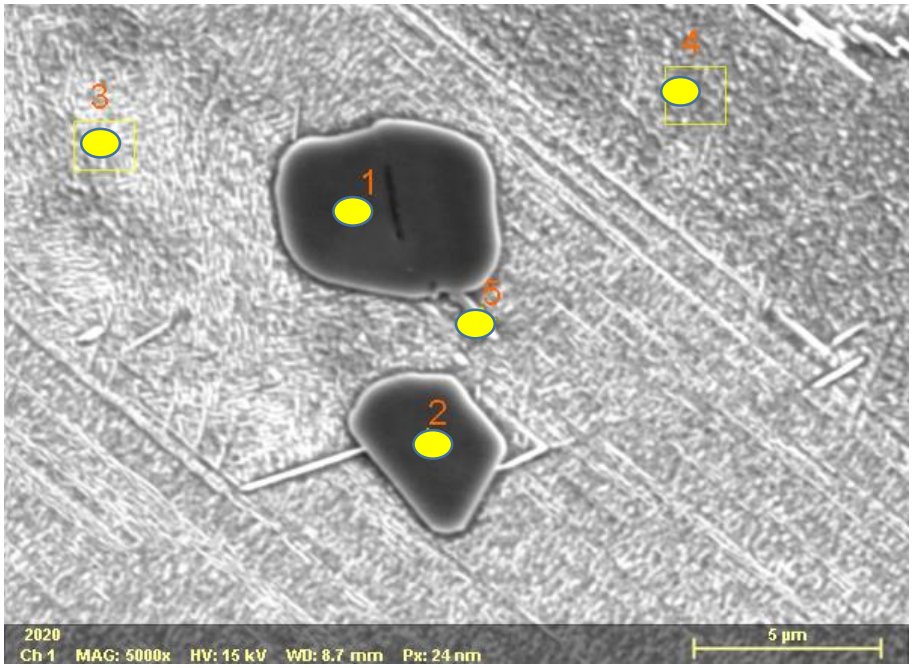

Fig 30. SEM micrograph of specimen IN_S taken at 5000X for EDS

The EDS data obtained by the secondary spectrums is given in below table.

Table 10. EDS data of block specimen IN_S

Spectrum	C	Al	Ti	Cr	Fe	Ni	Nb	Mo
1	17.74	0.04	3.66	0.29	0.26	1.36	71.84	4.81
2	19.77	0.07	3.29	0.42	0.53	1.33	69.82	4.78
3	8.60	0.45	1.06	16.71	17.41	47.14	5.57	3.06
4	8.43	0.48	0.89	16.94	17.30	47.20	5.50	3.25
5	6.20	0.00	1.35	17.45	17.92	49.27	4.49	3.32

From the EDS analysis, the presence of Nb rich carbides are confirmed. Spectrum 3, 4 and 5 show that Nb % is below 6% in those areas which indicates the presence of gamma double prime in those areas. Al and Ti contents are sufficiently low which confirms that the presence of Ni_3 (Al, Ti) phase is not as high as the Ni_3Nb phase. The standard specimen is mainly strengthened by gamma double prime.

4.2 Tensile test

4.2.1 Room temperature tensile tests

The tensile specimen were undergone both room temperature and high temperature tests. The high temperature tests were performed at 650°C with a strain rate of 10^{-3} mm/sec. The room temperature tensile test data of the samples heat treated at different temperature is given in the below table-

Table 11 – Room temperature tensile data

Specimen name	Heat treatment temperature (°C)	Diameter (mm)	Area (mm^2)	Elongation (%)	Yield strength (Mpa)	Ultimate tensile strength (Mpa)
IN_1RT	650°C (75 hours) + 620°C (8 hours)	6.03	28.56	42.55	821.45	1158.43
IN_2RT	750°C (75 hours) + 620°C (8 hours)	6.03	28.56	31.95	875.42	1245.21
IN_3RT	800°C (75 hours) + 620°C (8 hours)	6.033	28.58	32.16	708.005	1173.87
IN_4RT	900°C (75 hours)	5.973	28.02	44.25	368.62	828.24
IN_SRT	720°C (8 hours) + 620°C (8 hours)	5.96	27.89	37.00	1029.99	1302.56

From the room temperature tensile data it has been found that the specimen heat treated at 900°C has lowest strength among all. Reason behind this is the formation of delta enormously which reduces the strength of the material.

a) Standard heat treated specimen

The specimen which was undergone standard heat treatment has the highest yield strength among all. Compared to other specimens which were tested at room temperature, it is found that YS and UTS increases considerably in this case. While the tensile strength is coming high, on the other hand the ductility of the specimen decreases compared to the other specimens.

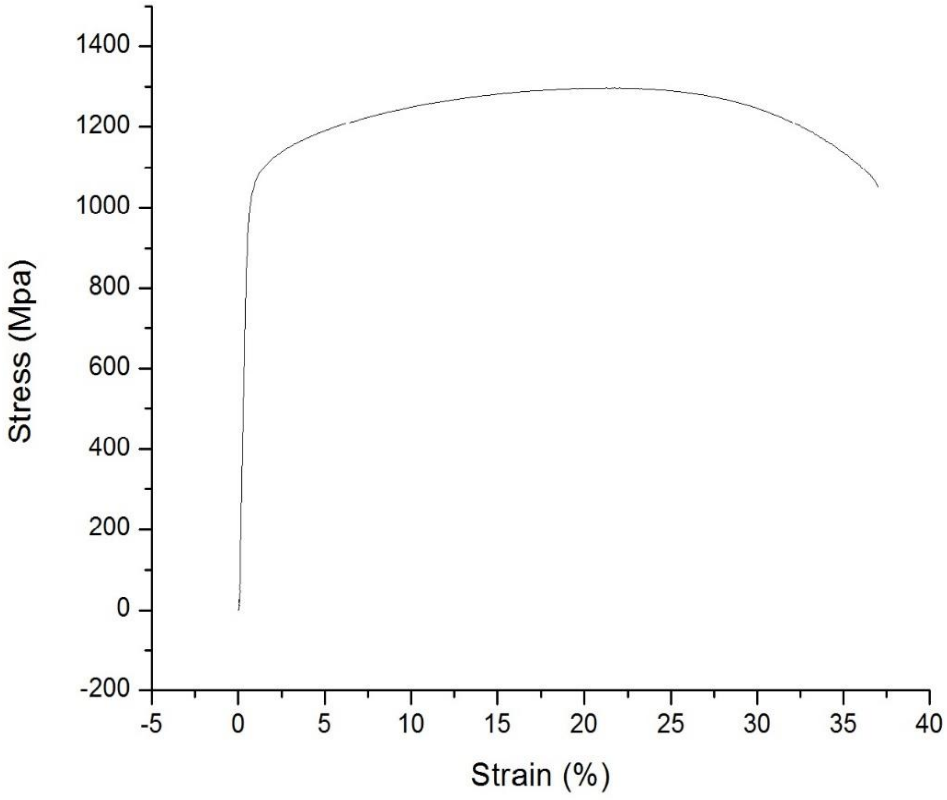

Fig 31. Stress – strain curve of standard heat treated specimen at room temperature

One of the major reason behind poor ductility of the standard heat treated specimens might be the high amount of gamma prime and gamma double prime which forms during heat treatment at 720°C and during age hardening the particles are cut off by dislocations by the precipitates. Another reason might be the precipitation of Niobium rich carbides at the particle grain boundaries during ageing which weakens the boundary and lowers the ductility of the material.

b) Specimens solution annealed at 1095°C

The room temperature tensile tests of the specimens solution annealed at 1095°C has shown comparatively higher ductility with the variety of quenching method applied on the specimens.

The specimen solution annealed at 1095°C and air cooled has shown greater ductility which was around 87% and the water quenched specimen elongated up to 83%. The room temperature tensile results of these specimens are given below-

Table 12 – Room temperature tensile properties of specimen solution annealed at 1095°C

Specimen name	Solution annealing temperature (°C)	Quenching method	Elongation (%)	Yield strength (Mpa)	Ultimate tensile test (Mpa)
IN_A	1095°C	Air	86.85%	282.819	716.66
IN_F	1095°C	Furnace	57.36%	668.91	1000.323
IN_W	1095°C	Water	83.48%	310.30	727.254

It can be seen from the tensile result that the specimen which was undergone furnace cooling possesses highest Yield strength and lowest ductility comparing with the other quenching methods. As the furnace cooling is the slowest cooling procedure among all of them, there are chances of consumption of large amount of Nb rich precipitates which enhances the strength properties but decreases the ductility. Though the air cooled specimen possesses high ductility, the strength of the specimen is very low compared to water cooling and furnace cooling. The stress – strain curve of the specimens tested at room temperature at a strain rate of 10^{-3} mm/sec and with the help of an extensometer of 12.5 gauge length and 100% travel is given below. In the following figure, Curve ‘a’ represents the specimen which was undergone furnace cooling, curve ‘b’ represents the specimen which was undergone air cooling and curve ‘c’ represents the specimen which was undergone water quenching.

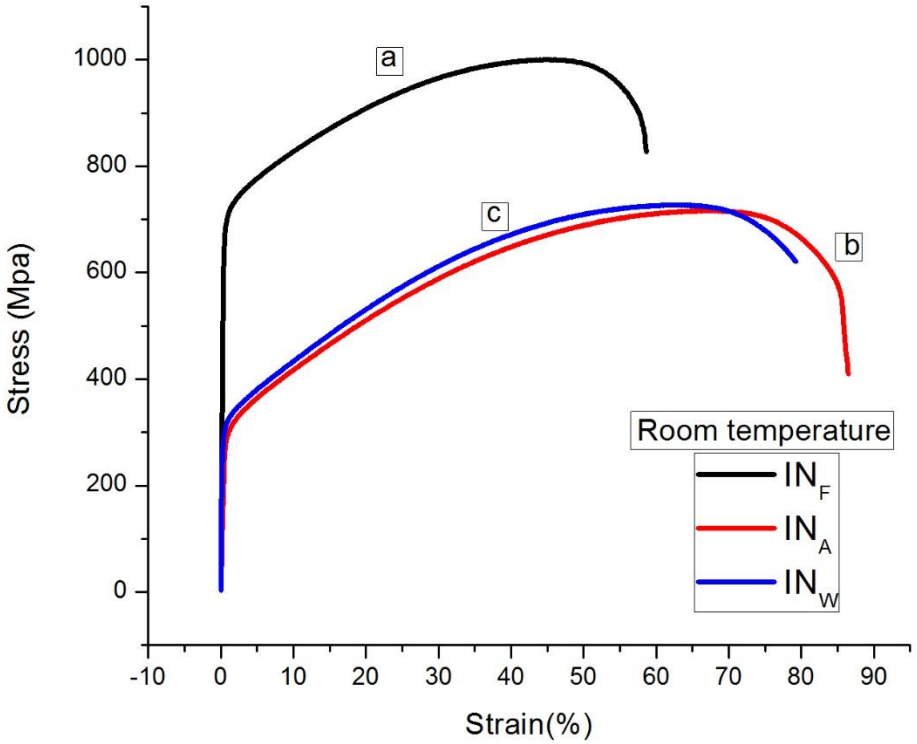

Fig 32. Stress – strain curve of specimen solution annealed at 1095°C

c) Specimens which are heat treated at different temperature after solution annealing.

The room temperature tensile tests were performed on the specimens which were heat treated at different exposure of temperature after solution annealing at 980°C followed by water quenching. From the result of room temperature test it can be seen that the specimen which was aged at 750°C has the highest strength with a YS value of 875 Mpa. This is due to the presence of gamma double prime which is a stable phase at 750°C and main strengthening phase of Inconel 718. At 800°C the gamma double prime is metastable phase and starts coarsening. And at the cost of gamma double prime the stable delta phase starts nucleating along grain boundaries and weakens the boundaries and as a result yield strength decreases to 708 Mpa. And at 900°C, due to rapid formation delta the strength also decreases considerably as the delta phase softens the material and hence causes increasing ductility. The stress strain curve for the aged specimens tested at room temperature is given in below figure.

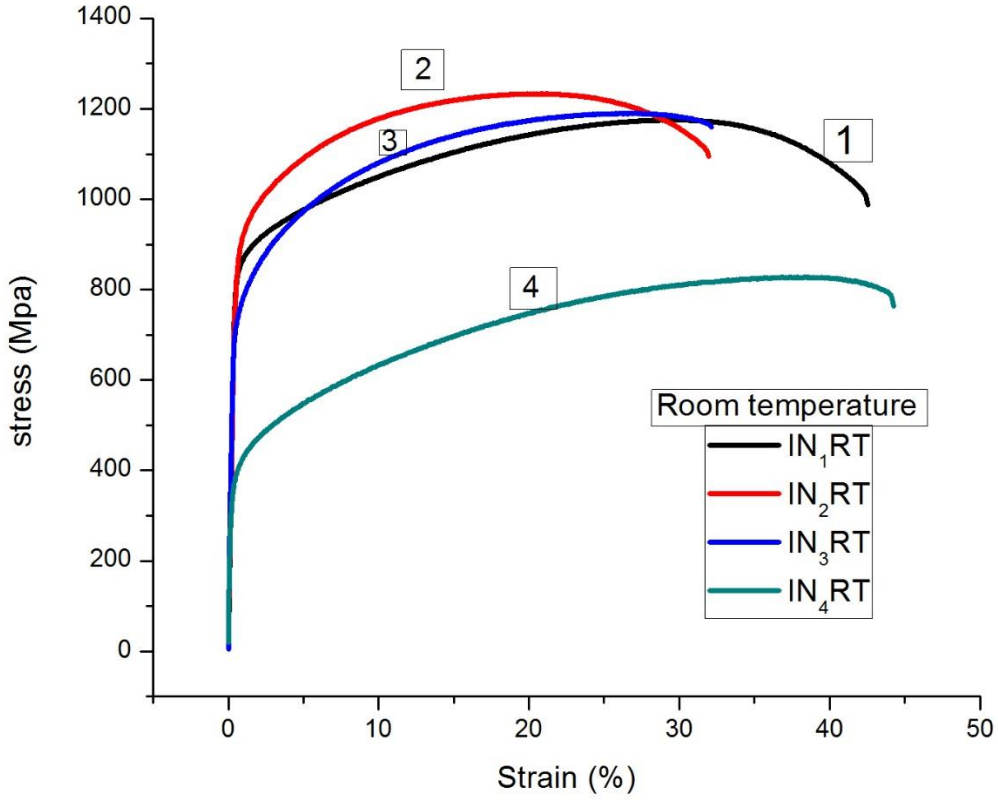

Fig 33. Stress – strain curve of specimens undergone ageing cycles

In the above figure curve 1 represents the specimen heat treated at 650°C for 75 hours at which the matrix phase remains there mostly with some gamma prime precipitates. That is why the elongation is well above 40%. Curve 2, 3, 4 accordingly represents the specimen aged at 750°C, 800°C and 900°C for 75 hours.

4.2.2 High temperature tensile test results

The high temperature tensile tests were performed at 650°C for all the specimen aged at different temperature and standard heat treated specimen as well. The result obtained from the tests are tabulated below. It is came to know that the high temperature behavior of the material is different from the room temperature. For some specimens, which had higher ductility at room temperature, at high temperature, the ductility became poor especially for the standard heat treated specimens.

Table 13 – High temperature tensile result of Inconel 718

Specimen name	Average diameter (mm)	Area $(mm)^2$	Elongation (%)	Yield strength (Mpa)	Ultimate tensile strength (Mpa)	Young's modulus (Gpa)
IN_1HT	6.07	28.94	17.25	838	1004.75	156.91
IN_2HT	6.03	28.56	30.556	763	964.145	247.547
IN_3HT	6.02	28.463	28.42	629.54	717.93	63.068
IN_4HT	6.04	28.652	25.92	476	579.23	133.102
$IN_{S1}HT$	5.95	27.80	8.85	925.55	1061.566	176.205
$IN_{S2}HT$	6.03	28.56	15.09	859.24	982.34	167.158
$IN_{S3}HT$	5.89	27.25	14.52	920.615	1068.705	178.50

At high temperature among all the specimens the standard heat treated specimens have shown greater strength as compared to the others and the sample aged at 900°C has poor strength among all. The stress strain curve of specimens aged at varying temperature is given below.

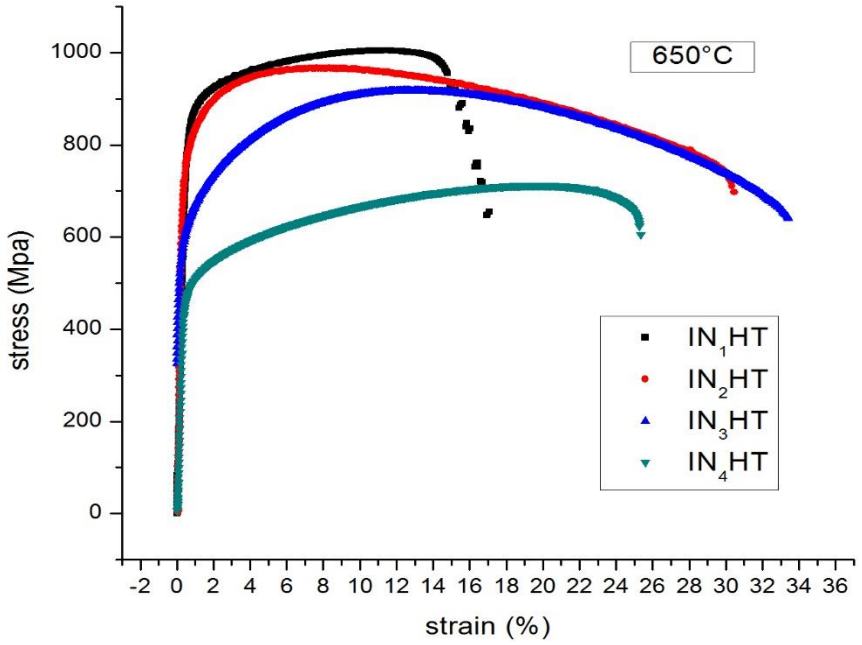

Fig 34. Stress – strain curve of specimen undergone ageing cycle

The reason behind the poor strength of the specimen aged at 900°C is the formation of delta which is a stable phase at that temperature and it softens the material and as a result

heterogeneous weakening of the material occurs and strength decreases. At 650°C, gamma prime and gamma double prime is a stable phase and being a major strengthening phase at this temperature the high temperature strength of the material is very high. But the ductility is poor at this this temperature as like the standard heat treated specimens. The stress – strain curve of standard heat treated specimen tested at 650°C is given in below figure-

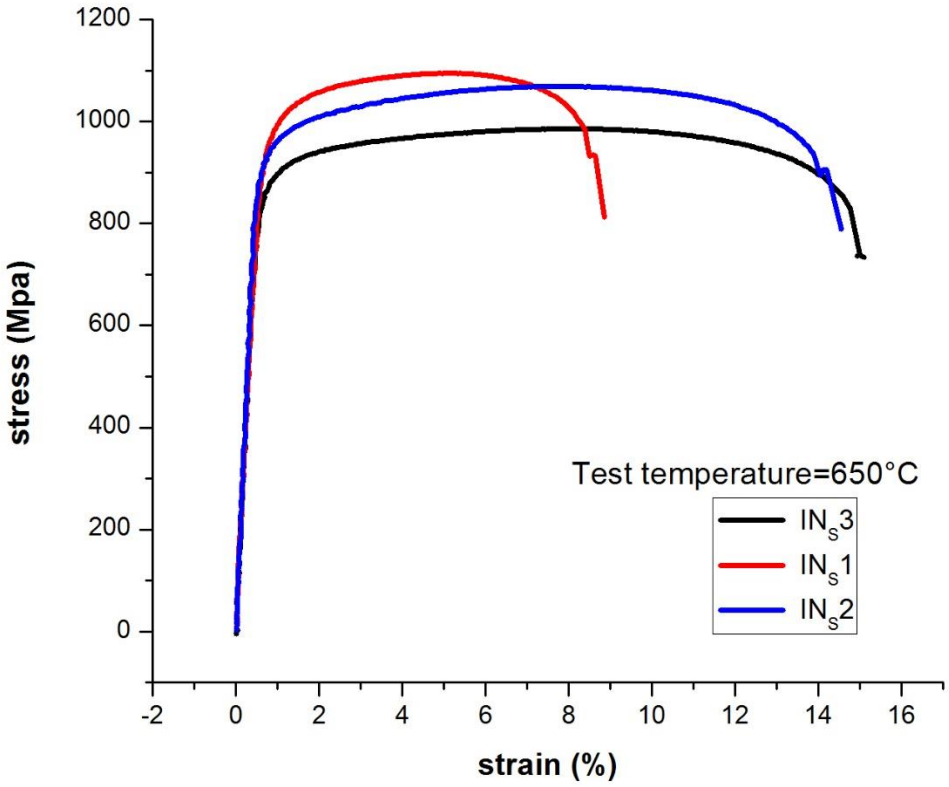

Fig 35. Stress – strain curve of standard heat treated specimen tested at high temperature

From the tensile test result of standard heat treated specimen it is came to know that compared to other specimens, ductility of these specimens is very low which has come around 15%. To make this sure repeated tests were performed but no major improvement noticed. The other sample had an elongation of 14.5%. From the microstructural analysis it has come to know that at around 720°C gamma prime and gamma double both exists in the matrix and strengthens it. Hence, the high strength at this temperature is desirable and from the test results it is found that yield strength is very high for the standard heat treated specimens. The reason behind poor ductility can be the formation of high amount of gamma double prime and gamma prime and carbides at grain boundary during heat treatment which causes cutting of the particles well before fracture so that the specimen can't elongate much. The bar graph of strength – ageing temperature for both room temperature and high temperature tensile test is given below.

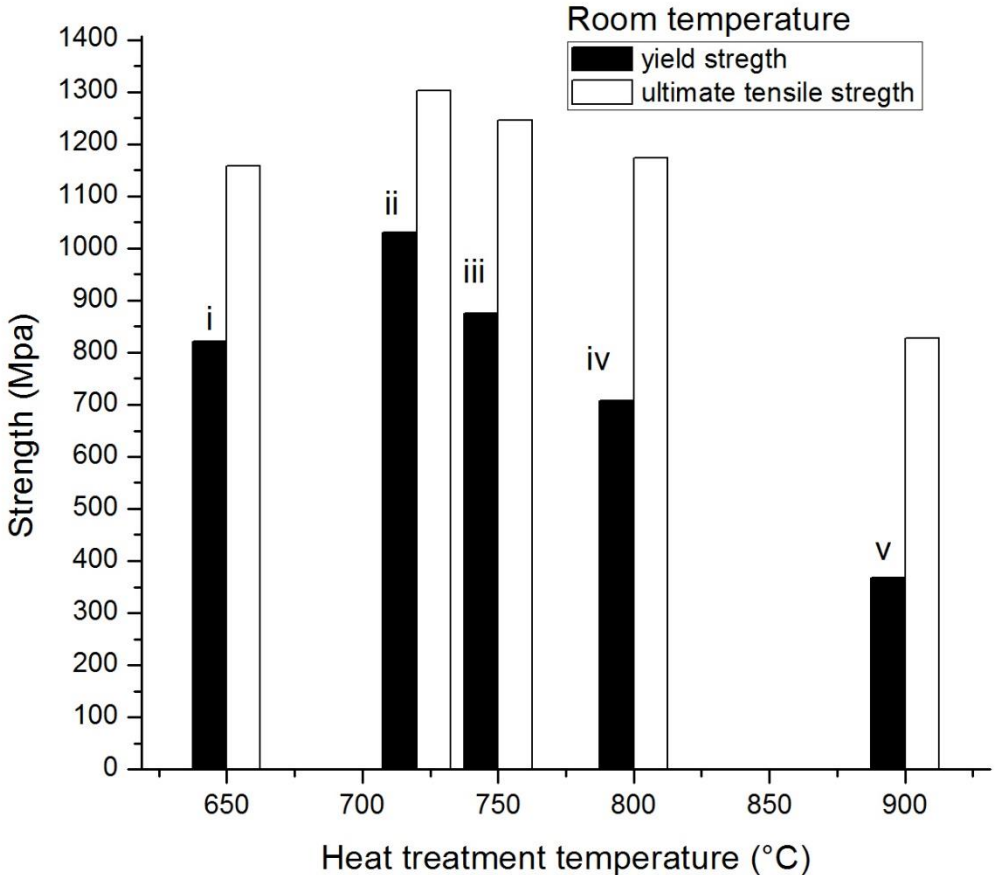

Fig 36. Bar graph of strength- heat treatment temperature for room temperature tests

In the above graph yield strength and ultimate tensile strength are plotted against the heat treatment temperature. (i) Indicates the YS and UTS of the specimen heat treated at 650°C. In the similar way (ii), (iii), (iv) and (v) represents the yield strength and ultimate tensile strength of the specimens heat treated at 720°C, 750°C, 800°C and 900°C. Specimen (ii) has highest YS and UTS among all. The bar graph of strength – ageing temperature for the specimens tested at high temperature is given below.

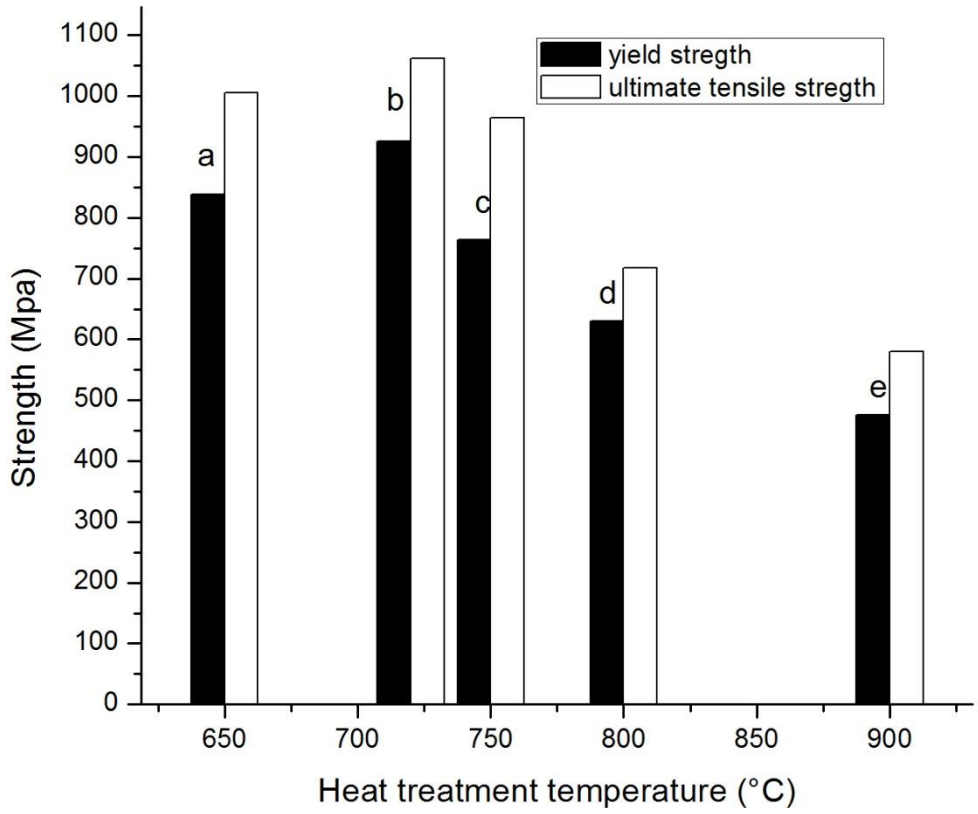

Fig 37. Bar graph of strength – heat treatment temperature for high temperature tests

In the above graph (a) indicates the YS and UTS of the specimen heat treated at 650°C for 75 hours followed by water quenching and (b), (c), (d) and (e) represents the specimen heat treated at 720°C, 750°C, 800°C and 900°C and all the samples were water quenched. It can be seen that at the high temperature also the standard heat treated specimen possesses highest strength which justifies the use of the material for industrial purpose at that temperature.

4.3 Fractography

The fracture surface of the specimens after room temperature and high temperature tensile tests were examined in a scanning electron microscope using the secondary electron detector and EDS of the fracture surfaces were also taken. The fracto-graphs of the specimens tested at room temperature is given in the below figure.

4.3.1 Fractographs of the both room temperature and high temperature tensile specimens

a) Specimen IN_1

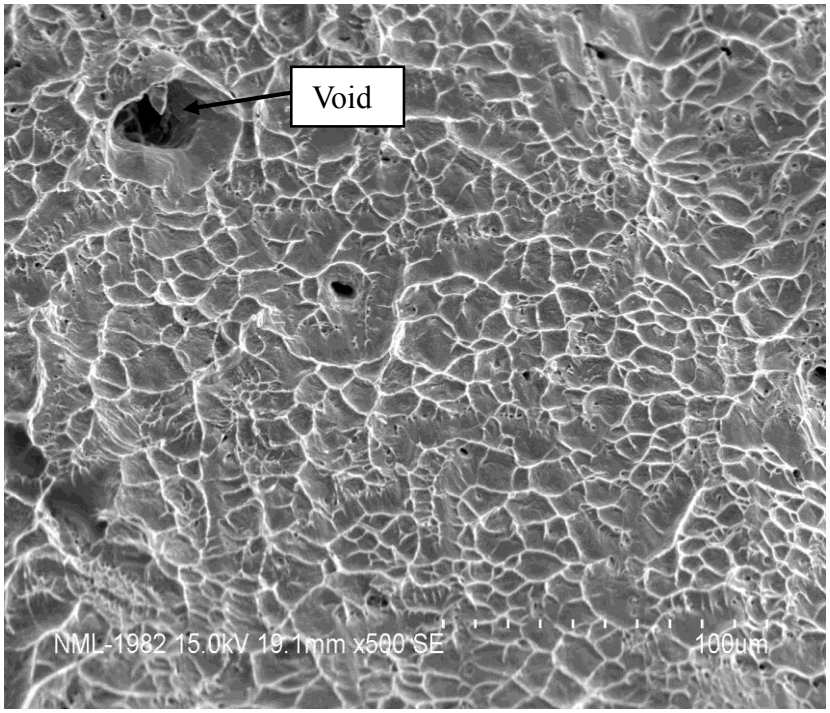

Fig 38. Fractograph of specimen IN_1 tested at room temperature

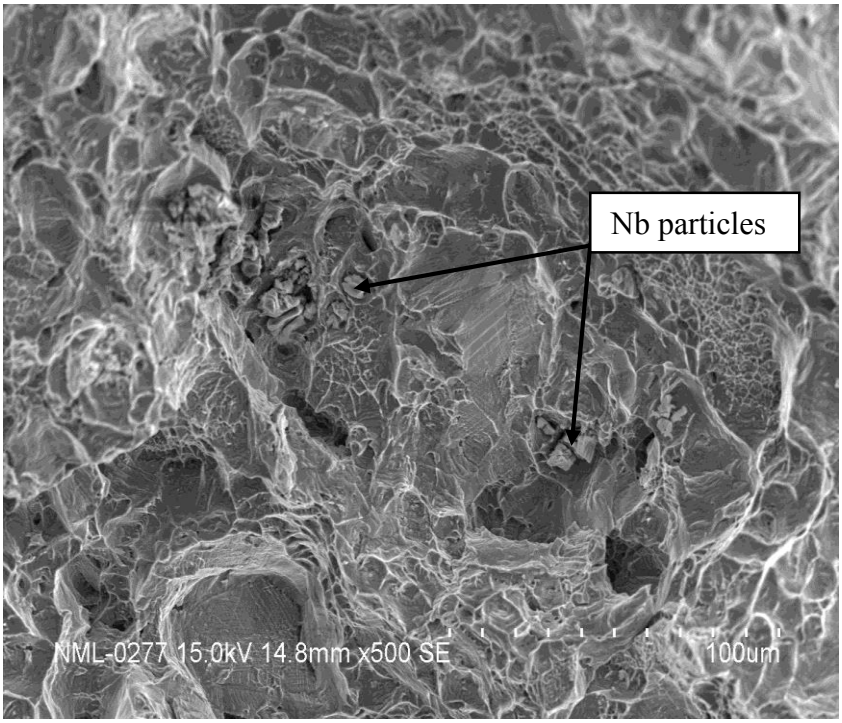

Fig 39. Fractograph of specimen IN_1 tested at 650° C

The fractograph taken by SEM of the specimen IN_1 when tested at room temperature shows particle boundaries and cup and cone like depression clearly, which indicates that the manner of failure of the specimen was ductile. And at high temperature the visibility of particle boundaries are not clear and from the surface morphology it can be seen that the failure manner

is less ductile than the room temperature tested specimen. The EDS analysis of the specimen is given below.

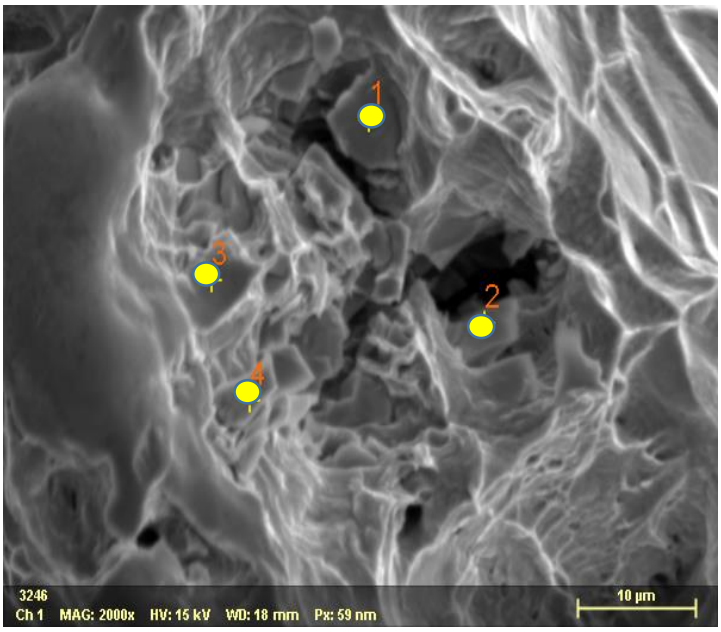

Fig 40. SEM image of the fracture surface of IN_1RT taken at 2000X for EDS

Table 14 – EDS data of specimen IN_1RT								
1	11.81	0.02	6.06	0.93	0.96	2.07	77.19	0.26
2	10.16	2.26	2.01	19.05	16.94	32.41	12.39	3.51
3	1.60	0.97	0.79	18.53	19.81	49.75	4.11	2.67
4	3.90	0.23	2.68	0.65	0.55	1.09	84.57	2.22

From the EDS data it has been found that spectrum 1 and 4 indicates the area which is highly Nb rich and the spectrum 2 and 3 indicates Ni rich area or the matrix material. The EDS analysis of the specimen undergone high temperature tensile test is given below.

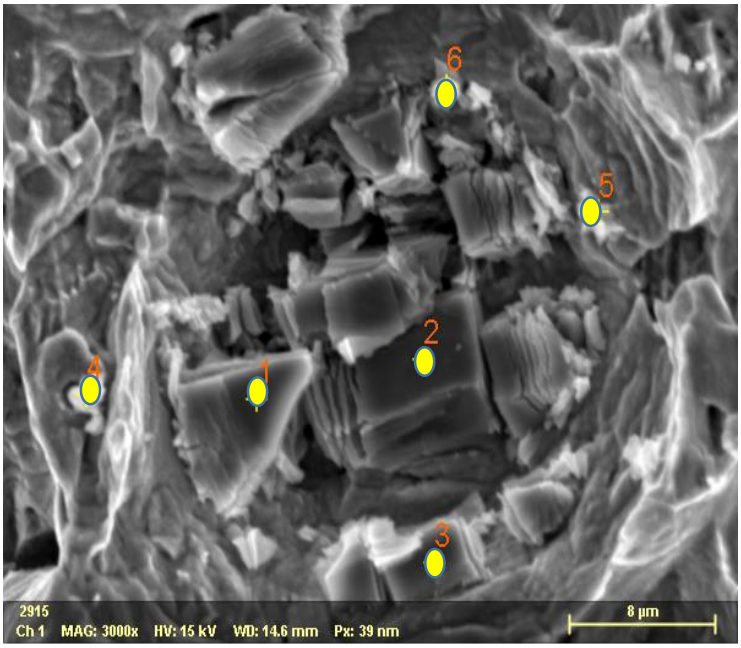

Fig 41. Fracture surface of IN_1HT taken at 3000X for EDS

The EDS data is given in below table-

Table 15 – EDS data of specimen IN_1HT

Spectrum	C	N	O	Ti	Cr	Fe	Ni	Nb	Mo
1	7.70	13.17	47.46	27.65	0.20	0.14	0.30	3.32	0.06
2	0.69	1.40	12.58	71.41	1.22	0.30	0.77	11.25	0.37
3	7.93	14.69	50.22	23.23	0.24	0.17	0.39	2.82	0.02
4	13.64	5.50	59.05	2.50	1.96	1.84	2.84	12.34	0.33
5	12.25	6.74	52.46	11.52	3.80	3.34	6.86	2.67	0.35
6	14.41	7.10	58.03	9.25	1.49	1.27	2.52	5.66	0.27

From the EDS data it is seen that at high temperature oxide formation has occurred enormously as the amount of O is sufficiently high in the regions 1,3,4,5 and 6. The spectrum 2 indicates the area which is Ti rich as the amount is very high. The chances of formation of TiN or TiC is high as it contains 12% C also. As the amount of Nb is lower in most the regions hence the ductility of the specimen is not much high as compared to the room temperature tested specimen.

b) Specimen IN_2

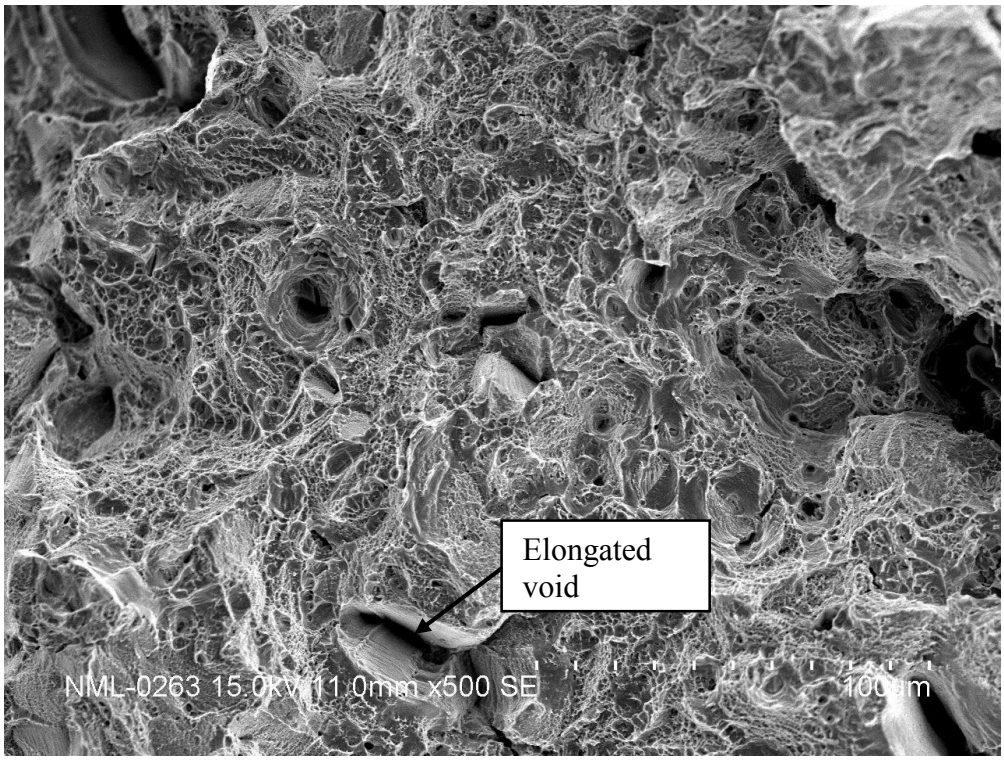

Fig 42. Fracture surface of specimen IN_2 tested at room temperature

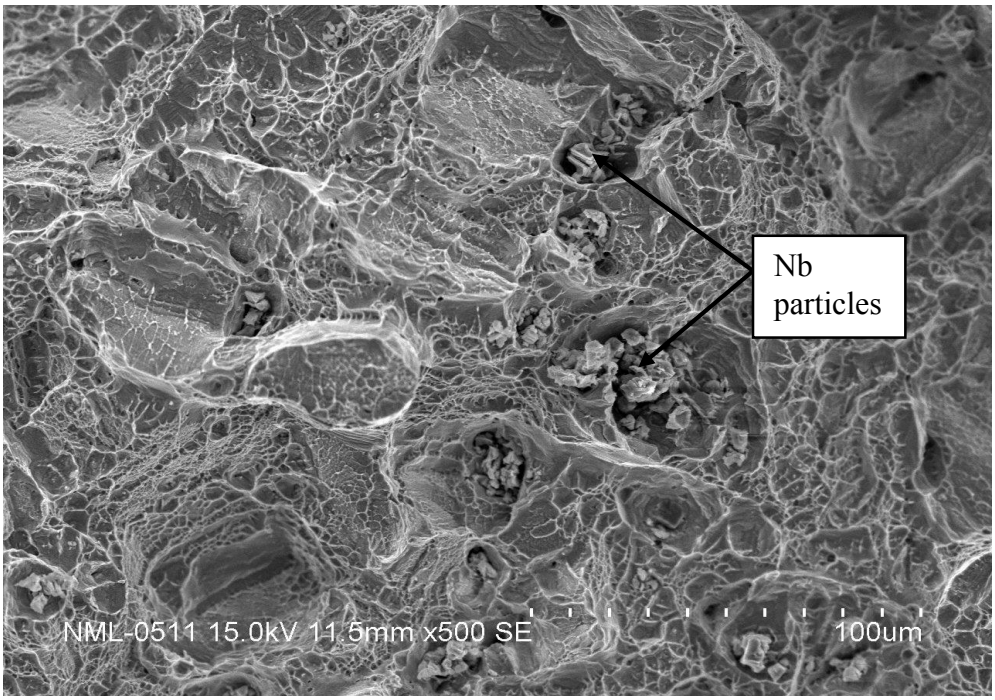

Fig 43. Fracture surface of specimen IN_2 tested at 650°C

The fracture surface of the specimen shows dimple ruptures at room temperature and high temperature both and a ductile fracture mode was observed for both the tested condition by the

cup – cone depression. At room temperature it is seen that at some places the micro-voids are elongated but at high temperature the mostly the voids are filled with intermetallic particles such as Ti or Nb. The EDS analysis of the specimens are given below.

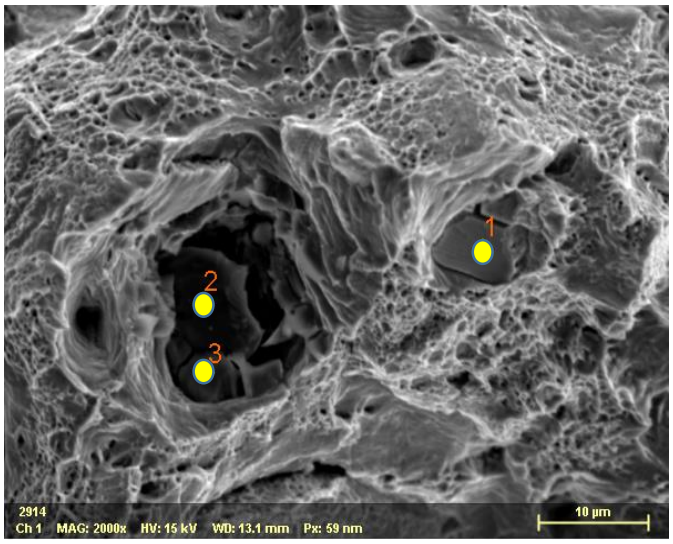

Fig 44. SEM image of IN_2RT taken at 2500X for EDS

The EDS data obtained by the secondary spectrums is given in below table-

Table 16 – EDS data of specimen IN_2RT

Spectrum	C	N	Al	Ti	Cr	Fe	Ni	Nb	Mo
1	55.19	15.75	0.14	4.24	0.91	0.89	1.89	20.83	0.18
2	14.48	39.73	0.10	38.75	0.62	0.43	0.79	5.05	0.06
3	1.89	1.19	0.00	82.81	2.06	1.63	3.19	6.79	0.46

From the EDS analysis it is seen that spectrum 1 indicates the region where the presence of Nb particle is observed. Spectrum 2 indicates the region where there is the presence of Ti and N both are high and the spectrum 3 indicates the region which is highly Ti rich and lesser Nb. The EDS analysis of the high temperature tensile specimen is given below.

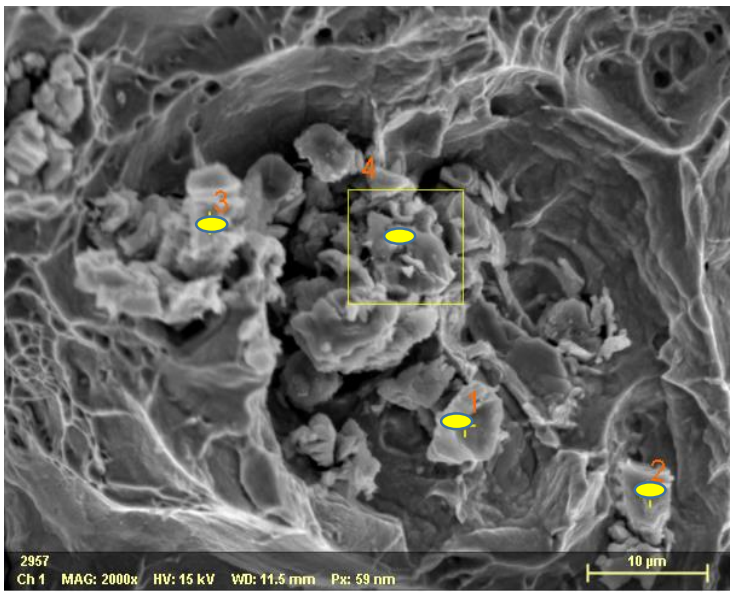

Fig 45. SEM image of IN_2HT taken at 2000X for EDS

The EDS data is given in the below table-

Table 17 – EDS data of specimen IN_2HT

Spectrum	C	N	Al	Ti	Cr	Fe	Ni	Nb	Mo
1	6.96	0.56	0.25	3.69	2.14	2.07	3.28	70.90	1.05
2	8.10	25.32	0.11	4.59	2.00	1.49	3.88	53.55	0.94
3	8.32	26.79	0.10	4.91	1.29	1.34	2.60	53.61	1.04
4	6.48	9.69	0.55	3.82	3.72	3.18	5.44	63.04	4.09

In the fractographs of high temperature tensile specimens it was seen that the voids were filled with some particles. By the EDS analysis it has been confirmed that those particles were mainly Nb particles. Here also the aluminum and Titanium content is very low. It can be said that gamma double prime formation at 750°C has taken place with the coarsening of gamma prime. As the sum of (Al + Ti + Nb) is very high, the specimen possesses good tensile strength. And at the room temperature and high temperature the ductility is almost same which is around 31%.

c) Specimen IN_3

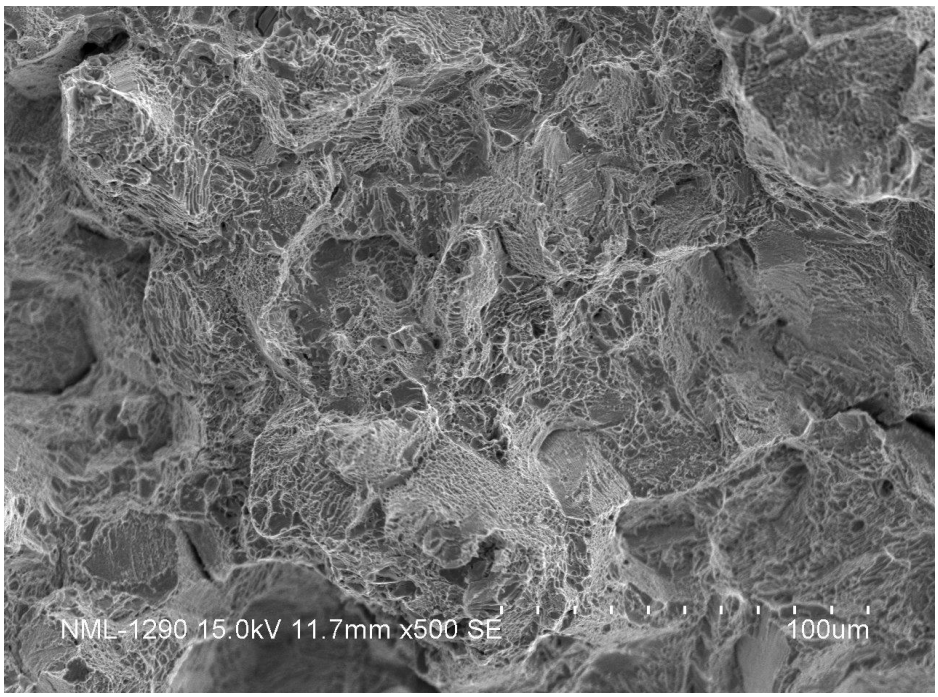

Fig 46. Fracture surface of specimen IN_3 tested at room temperature

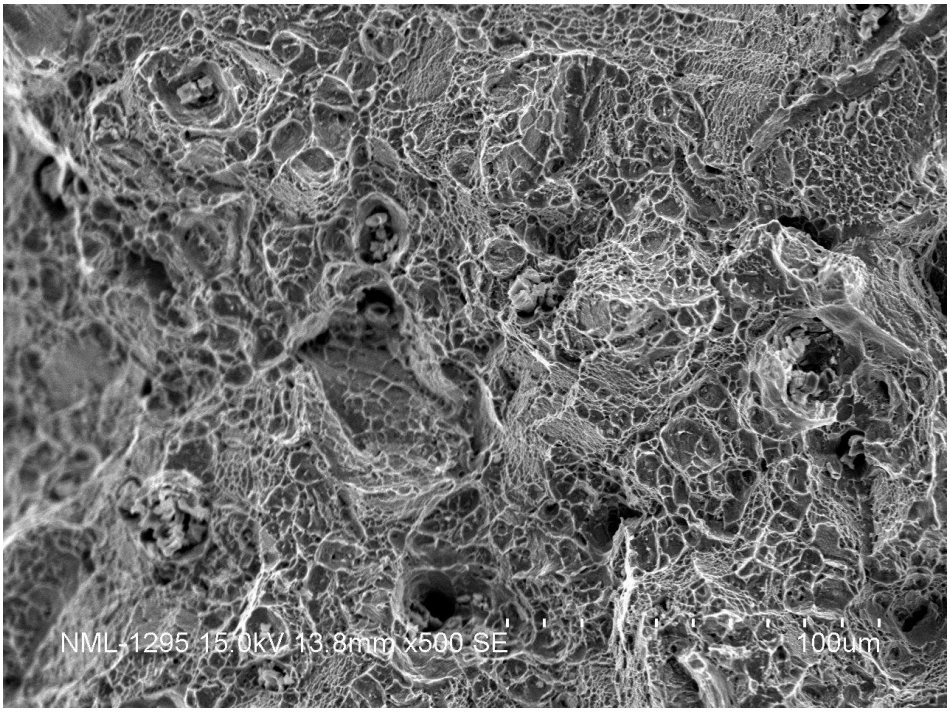

Fig 47. Fracture surface of specimen IN_3 tested at 650°C

From the fractographs of the tensile specimen which were heat treated at 800°C for 75 hours, it is seen that the formation of voids have become less at room temperature. The fracture surface

shows the dimples covered most of the areas confirming that the mode of fracture is definitely ductile as like the specimen heat treated at 750°C. The dimples are smaller in area compared to the previous specimen's fracture surface. There are some inclusions inside the micro-voids. To know the morphology and composition of the inclusions EDS results are described below-

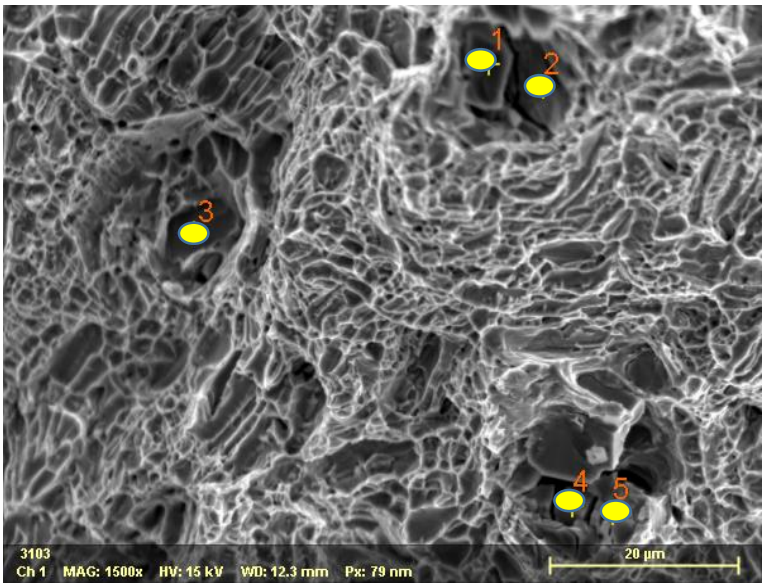

Fig 48. SEM image of IN_3RT taken at 1500X for EDS

The EDS data of the specimen IN_3RT is tabulated below.

Table 18 – EDS data of specimen IN_3RT

Spectrum	C	N	Ti	Cr	Fe	Ni	Nb	Mo
1	9.32	19.69	54.52	0.96	0.43	0.84	13.90	0.34
2	7.95	21.33	51.62	1.27	0.75	2.57	14.52	0.00
3	1.82	0.54	71.50	3.75	3.00	6.67	9.76	2.97
4	6.53	2.23	36.14	3.03	2.71	6.52	41.70	1.09
5	7.07	1.08	7.78	2.58	1.97	5.45	71.62	2.24

From the EDS data it is came to know that the inclusions are mostly Titanium or Niobium particles which presents there along with some amounts of Nitrogen and carbon and is responsible for the formation of TiN or NbC phases. As higher Ti content favors gamma prime formation, in this case from the spectrums it has been found that the amount of Titanium is sufficiently high which ensures the presence of gamma prime phase. That is why strength is

sufficiently high at this temperature but lesser than the specimen aged at 750°C. From microstructural analysis it is already obtained that at 800°C the major strengthening phases starts to coarsen and cause a slight decrease in strength. The EDS analysis of the specimen IN_3 tested at high temperature is given below.

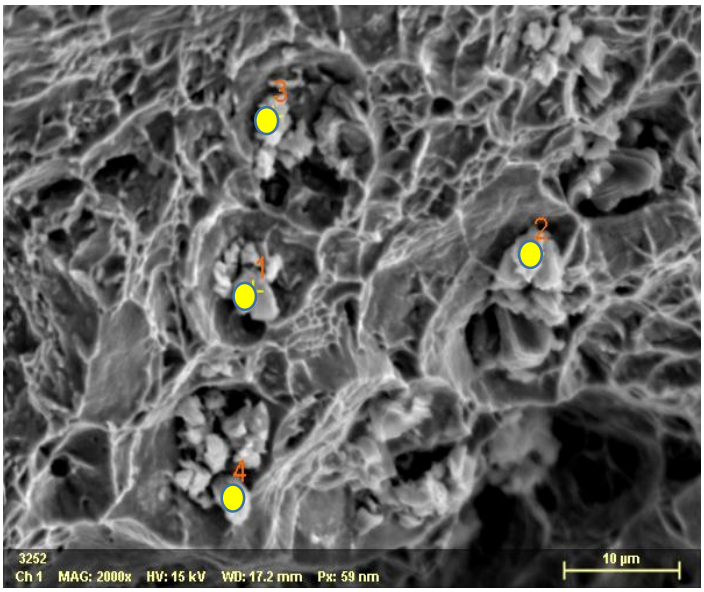

Fig 49. Fracture surface of IN_3HT taken at 2000X for EDS

The EDS data that has been acquired by the x ray spectrums is given in below table.

Table 19 – EDS data of specimen IN_3HT

Spectrum	C	Ti	Cr	Fe	Ni	Nb	Mo
1	7.54	6.79	5.64	5.18	10.68	62.92	1.26
2	5.27	7.16	4.53	4.26	8.48	68.73	1.55
3	9.60	8.86	4.72	4.11	8.54	63.11	1.06
4	4.35	3.02	12.14	11.67	31.85	34.21	2.76

From the EDS analysis, it is found that the particles that filled the voids are mostly niobium particles and from the table it is ensured that (Ti + Nb)% is also high which indicates that the specimen possesses god strength at this temperatures.

d) Specimen IN_4

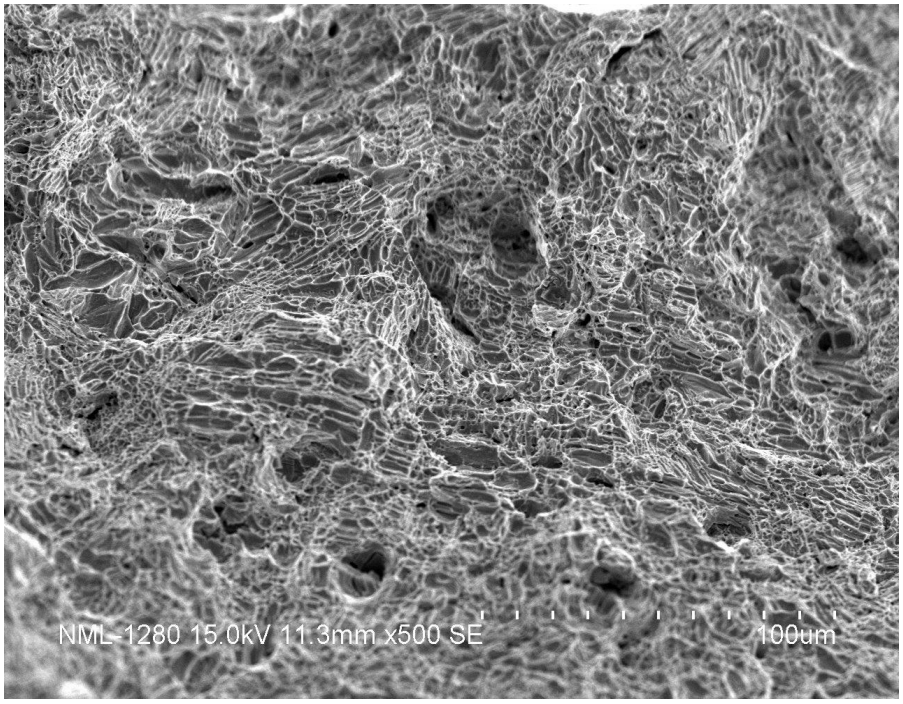

Fig 50. Fracture surface of specimen IN_4 tested at room temperature

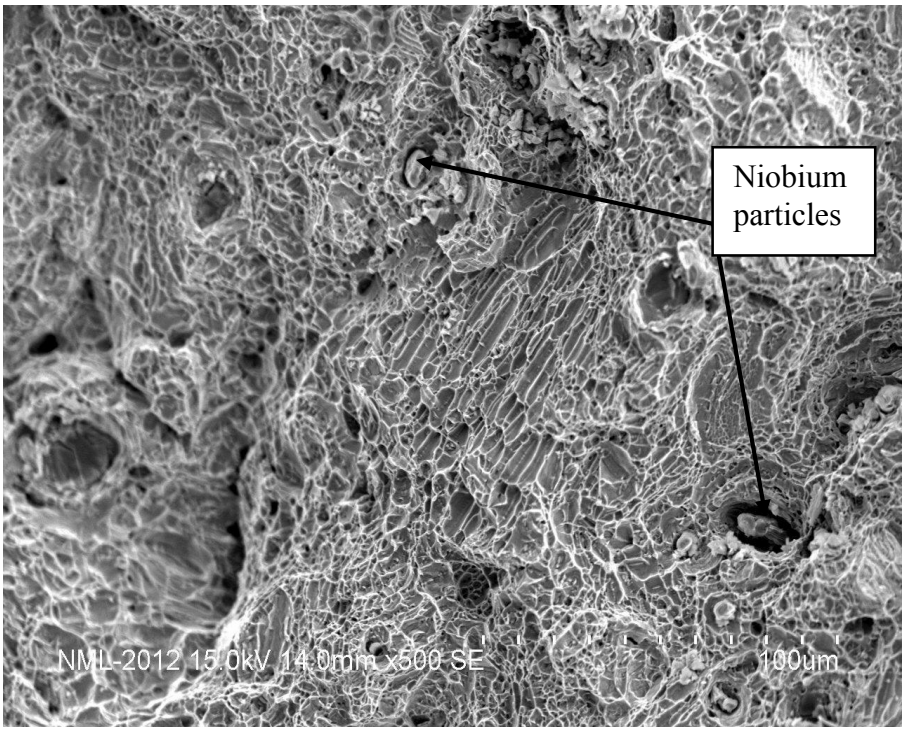

Fig 51. Fracture surface of specimen IN_4 tested at 650°C

From the fractographs it can be seen that, for the high temperature tensile specimen the dimples are not uniformly distributed over the surface area which indicates that at high temperature the

mode of failure is not fully ductile. From the stress-strain curve it is found that strength has become poor for these specimens. By EDS analysis the presence of the desired phase at this temperature which is delta phase is ensured.

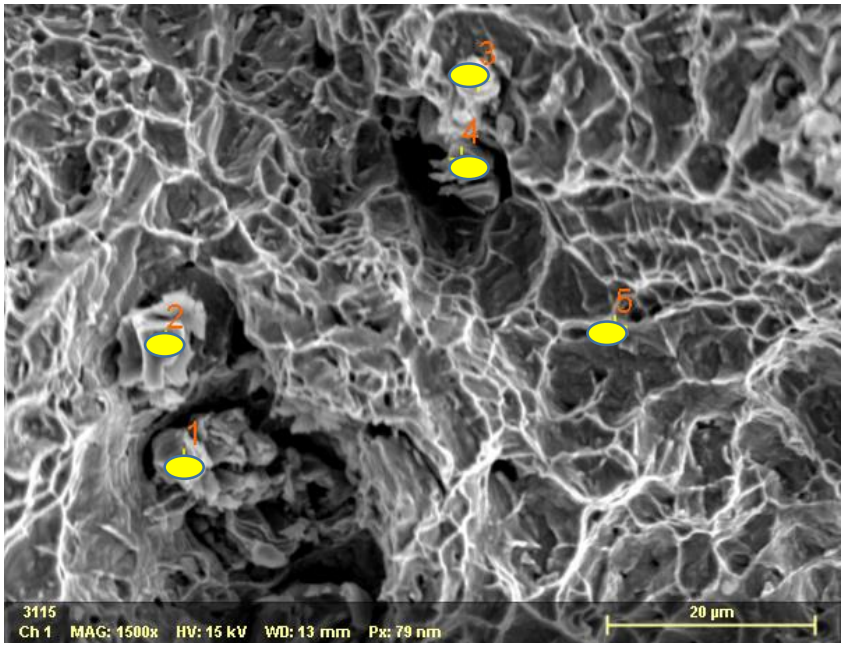

Fig 52. Fractograph of the specimen IN_4RT taken at 1500X for EDS

The EDS data is tabulated below-

Table 20 – EDS data of specimen IN_4RT

Spectrum	C	N	O	Al	Ti	Cr	Fe	Ni	Nb	Mo
1	2.88	1.51	10.75	0.15	2.91	2.22	2.22	4.45	71.29	1.61
2	6.85	2.75	28.18	0.08	4.78	0.88	0.77	1.91	53.28	0.43
3	5.38	1.26	20.70	0.03	4.36	1.67	1.53	3.58	60.88	0.60
4	5.30	0.60	18.54	0.70	7.59	2.45	2.19	3.35	57.94	0.88
5	7.74	2.01	12.03	0.31	0.81	17.45	16.59	37.44	3.20	2.31

The EDS data shows that most of the inclusions of the voids are Nb particles. And the amout of niobium is sufficiently high which assists in the formation of delta. The high temperature EDS result is given below.

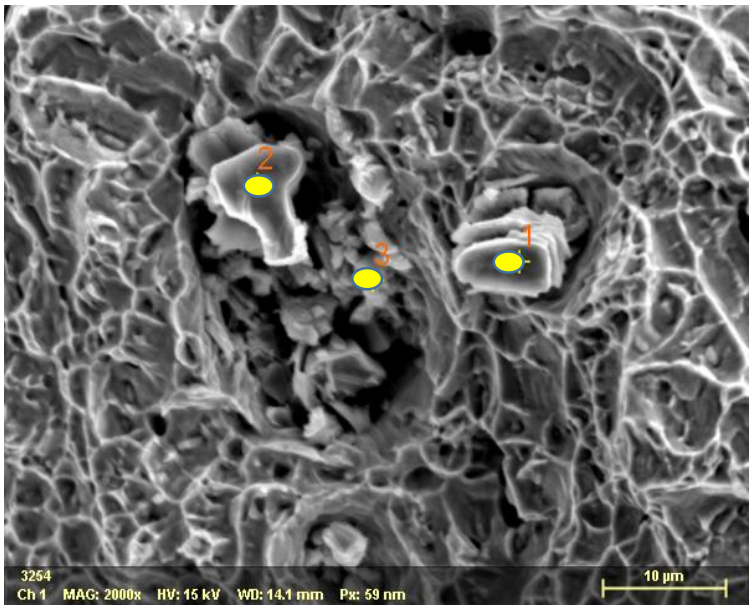

Fig 53. Fractograph of IN_4HT taken at 2000X for EDS

The EDS data is given in below table-

Table 21 – EDS data of specimen IN_4HT

Spectrum	C	Ti	Cr	Fe	Ni	Nb	Mo
1	9.34	8.16	1.38	1.32	1.76	76.87	1.17
2	7.64	3.70	1.15	0.84	2.11	82.13	2.43
3	10.72	5.16	5.18	4.41	9.30	64.88	0.35

From the EDS data of high temperature tensile specimen it is came to know that the amount of Nb content is very high and the amount of Al is so low that it can be ignorable. The ratio of (Al + Ti)/Nb is also coming low. Hence, the formation of delta at this temperature can be assured. Being a softer phase it decreases the strength of the material as the strength analysis at high temperature has shown this specimen has poor yield strength compared to other aged specimens. This happens due to the brittle delta particles in the matrix.

e) Specimen INs

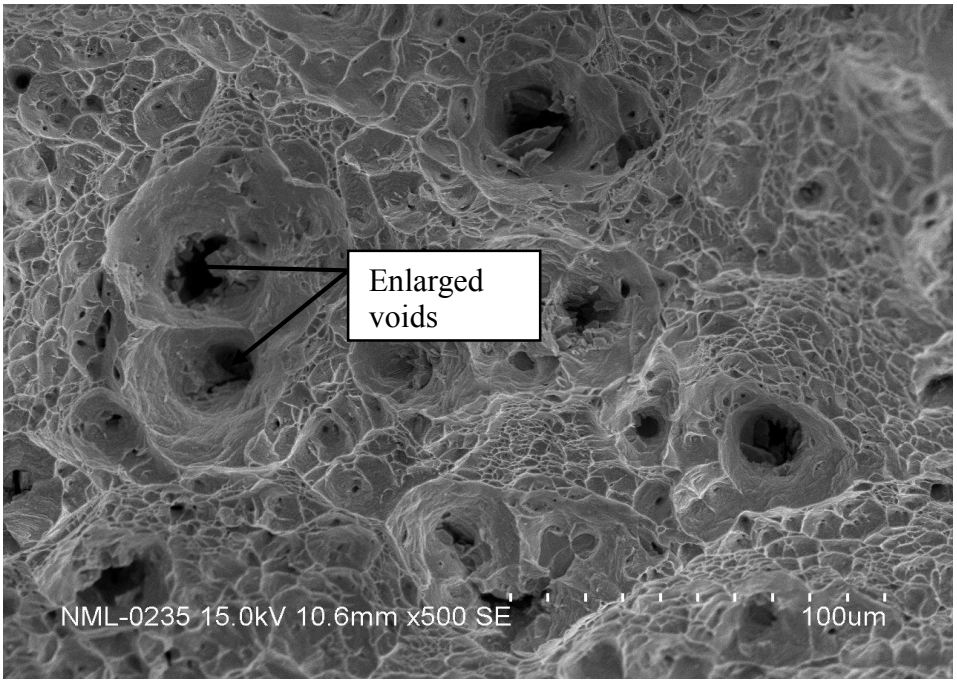

Fig 54. Fracture surface of IN_S tested at room temperature

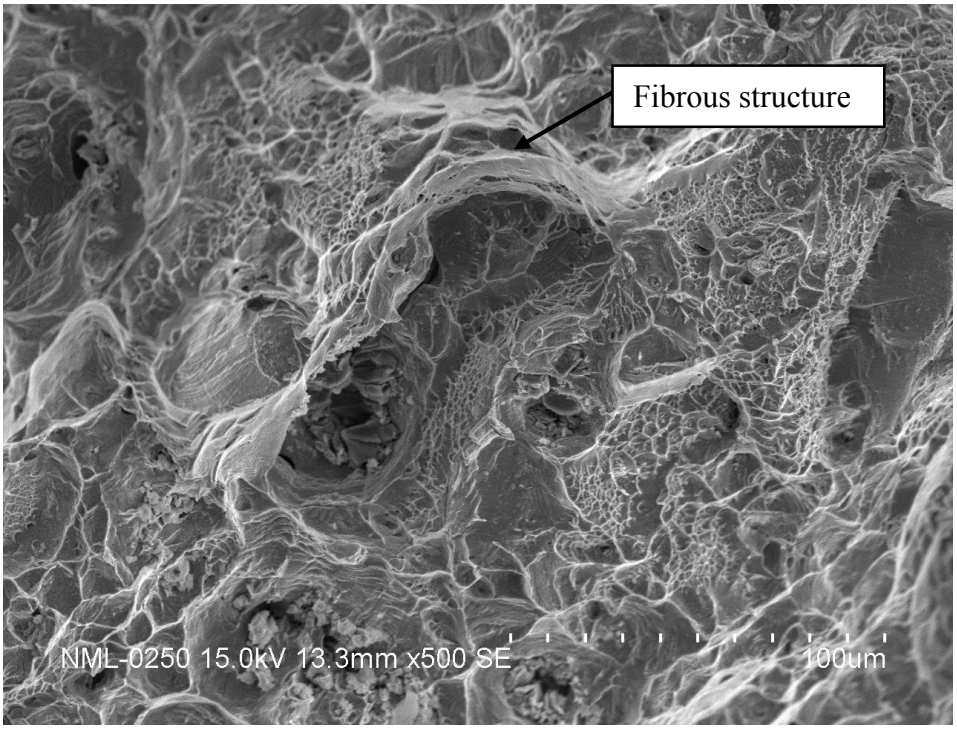

Fig 55. Fracture surface of specimen IN_S tested at 650°C

Fractographs of standard heat treated tensile specimens reveals fine dimple structures inside the coarse grains and boundaries of the particles. The room temperature tested specimen has shown the distribution of micro voids over the surface or the matrix. But at high temperature

the voids are mostly filled up by precipitates. The constituents of the precipitates are characterized by EDS which is given below.

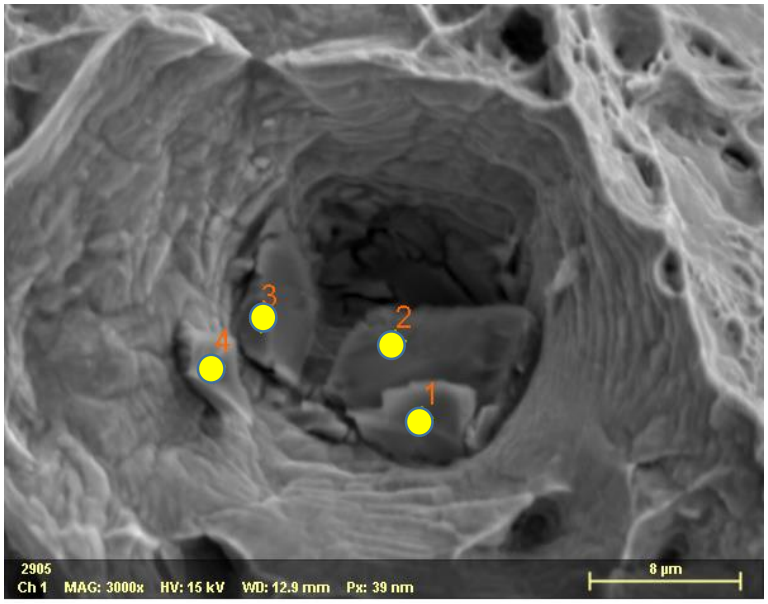

Fig 56. Fractograph of IN_SRT taken at 3000X for EDS

The EDS data obtained by four spectrums is given in below table.

Table 22 – EDS data of specimen IN_SRT

Spectrum	C	N	Al	Ti	Cr	Fe	Ni	Nb	Mo
1	10.90	2.84	3.13	69.22	5.40	2.86	3.59	1.40	0.67
2	27.80	3.58	0.66	30.01	10.57	10.05	16.11	0.97	0.26
3	18.03	0.00	1.75	66.05	5.20	2.86	4.97	0.87	0.29
4	16.38	38.64	0.20	35.34	1.55	1.16	2.42	4.31	0.02

The EDS result is showing that amount of Ti is very high in the precipitate which is present there as an inclusion of void. As higher Ti content favors gamma prime formation, the presence of gamma prime is for sure in the surface but as the amount of Nb is very low there is not much influence of gamma double prime which causes good ductility at room temperature around 37%.

The EDS analysis of high temperature tensile specimen is given below.

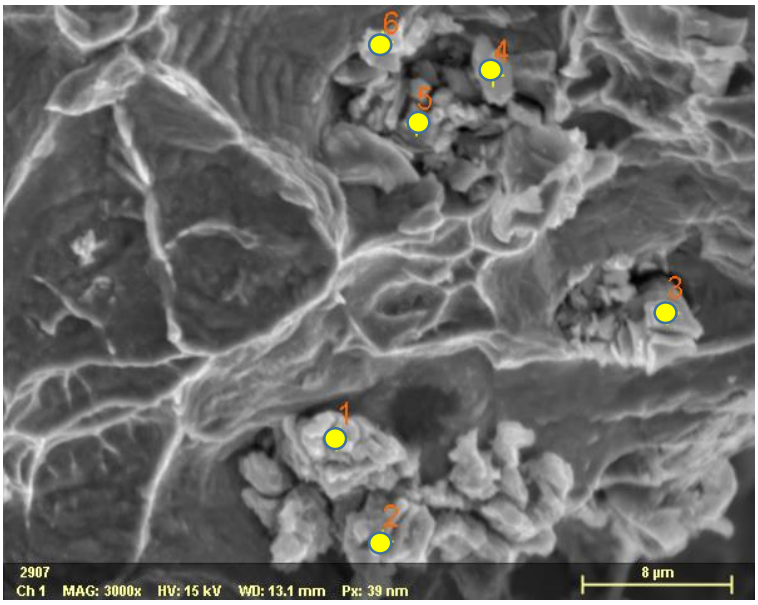

Fig 57. Fracture surface of IN_SHT taken at 3000X for EDS

The EDS data is given in below table-

Table 23 – EDS data of specimen IN_SHT

Spectrum	C	O	Al	Ti	Cr	Fe	Ni	Nb	Mo
1	20.73	58.82	0.10	2.22	1.51	1.19	1.95	13.48	0.00
2	22.45	52.91	0.10	3.05	2.15	1.59	2.80	14.95	0.00
3	20.56	55.83	0.13	3.57	1.36	1.14	2.08	15.32	0.00
4	19.06	58.41	0.14	2.05	1.44	1.14	2.39	15.32	0.04
5	12.35	28.21	0.46	5.50	1.64	1.81	3.39	46.13	0.52
6	22.85	54.84	0.25	1.77	2.29	2.07	3.56	12.25	0.12

The EDS analysis of the standard specimen tested at high temperature revealed that oxide formation has taken place and precipitation of carbides for sure as the carbon percentage is high which causes weakening the grain boundaries. Ti content decreases and Nb content increases which means the stability of gamma prime at this temperature decreased and the micro-voids are influenced by the major strengthening precipitate gamma double prime. From the microstructural analysis it has been found that growth of gamma double prime occurs in between 650-750°C. Hence, at 720°C the growth of gamma double prime occurs and starts deforming inside the interior of the micro voids which results in deformation of the material

well before fracture which is called premature fracture. That is why ductility of the standard heat treated specimens became poor.

4.4 Hardness test result

The Vicker's macro-hardness test result is given in below table.

Table 24- Vicker's Macro hardness test result

Specimen Name	Ageing Temperature (°C)	Hardness Value at each indentation (HV_{30})					Average Hardness (HV_{30})
		1st	2nd	3rd	4th	5th	
IN_1	650°C (75 Hours) + 620°C (8 Hours)	388.5	393.0	402.0	396.0	414.0	398.7
IN_2	750°C (75 Hours) + 620°C (8 Hours)	366.0	361.5	375.0	376.5	371.4	370.7
IN_3	800°C (75 Hours) + 620°C (8 Hours)	340.5	339.0	333.0	334.5	336.0	336.6
IN_4	900°C (75 Hours)	216.0	219.0	216.0	213.0	216.0	216.0
IN_0	980°C (1 Hour)	165.0	166.5	169.5	171.0	166.5	167.7
IN_O	1095°C (1 Hour)	148.5	150	145.5	150	151.5	149.1
As received	Not heat treated	319.5	330.0	330.0	327.0	331.5	327.5

From the hardness test result it is found that among the aged samples post solution annealing the specimen aged at 900°C possesses lowest hardness. Reason behind this is at this temperature delta phase forms which contains large amount of Nb as constituent which softens the material. Hence, hardness comes poor but ductility is good. And the matrix gamma which has a FCC crystal structure, being a soft phase possesses low hardness as all the strengthening phases are dissolved in the matrix. The bar graph of hardness v/s ageing temperature is given below.

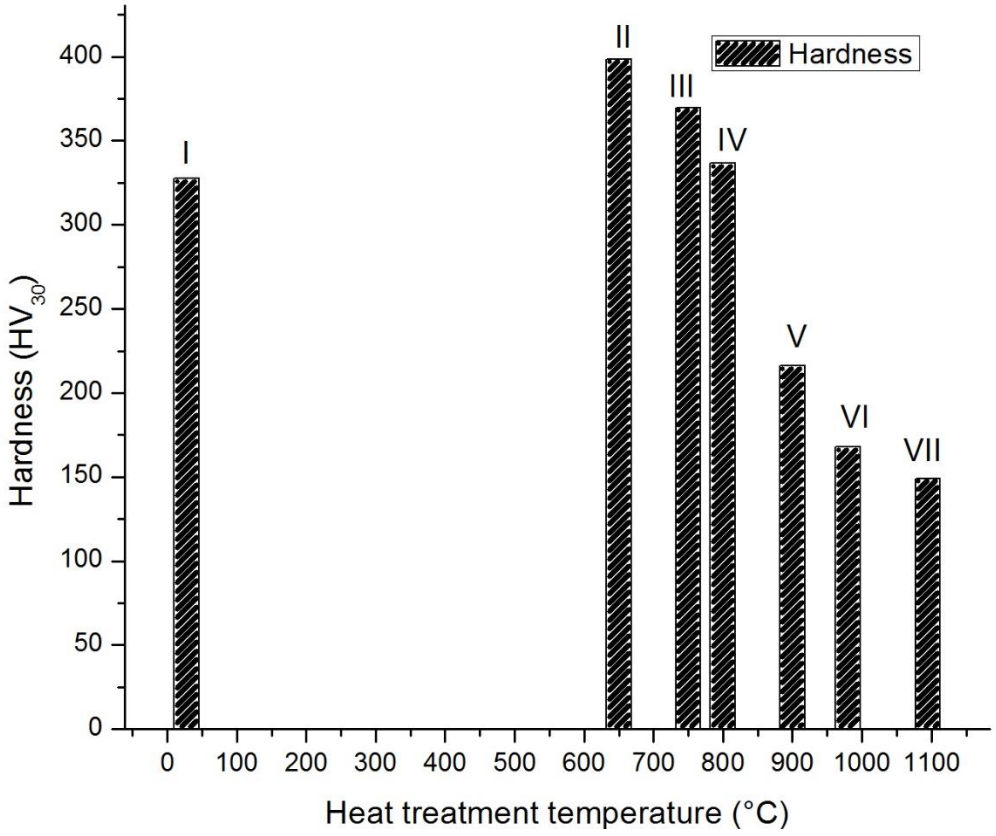

Fig 58. Bar graph plotted between hardness and ageing temperature

From the bar graph (II) indicates the hardness value at 650°C, (I) indicates the hardness value of as received specimen and (III), (IV), (V), (VI) and (VII) represents the hardness value accordingly of heat treated specimens from 750°C to 1095°C. At 1095°C the hardness value is very less as at this this temperature Nb particles dissolutes and hence the material becomes softer. It is seen that hardness decreases when the heat treatment is done at higher temperature.

Chapter 5. Conclusion

5.1 Conclusion

The conclusions that can be drawn from the performed experiments are as follows:

1. Ti and Al favors the formation of gamma prime rather that gamma double prime. Increases in (Al + Ti)/Nb ratio will increase the gamma prime formation. As it is coherent with the matrix the ductility is as high as solution annealed specimens. 750°C is the ageing temperature at which the major strengthening phase gamma double prime is stable and exists in large volume fraction in the matrix and that is why the strength is high at this temperature. Above this temperature the formation of delta needles are observed and it occupies the whole matrix at 900°C resulting poor strength of the material as they nucleates along grain boundaries and weakens the material. Delta formation can be resist lowering the Nb content as Nb is a major constituent of delta particles.
2. The double aged specimens are ideal for industrial use due to their high strength at high temperature which is caused by the stability of main strengthening phase gamma double prime at this temperature. The Nb content is not much high but still double aged specimens show poor ductility because of the nucleation of gamma double prime inside the micro-voids which results in premature failure of the specimen.
3. With increasing temperature the change in morphology of fracture surface observed and it can be concluded that the dimple size decreases at higher temperature which signifies that the ductility decreases as coarsening of precipitates occurs at higher temperature.
4. Hardness decreases with increasing temperature and attains a low value at 900°C where delta forms which softens the material. Hardness value depends on quenching methods as well. The oil quenched specimen possesses lower hardness compared to water quenched. This might happen as the growth of the precipitates resisted by rapid quenching.

References

[1] El-bagoury, N., & Ramadan, Heat Treatment Effect on Microstructure and Mechanical Properties of Re-Containing Inconel 718 Alloy. 2012(September), 924–930.

[2] Yamamoto, K., & Ogi, Effect of rhenium on solidification of Inconel 718 alloy.

[3] Han, V. (1983). Strengthening super alloy mechanisms in Inconel 718. 17(March).

[4] Groh, J. R., & Radavich, J. F. (1991). Effects OF Iron, Nickel, and Cobalt on Precipitation Hardening of Alloy 718.

[5] Mahadevan, S., Nalawade, S., Singh, J. B., & Verma, A. (2010). Evolution of δ phase Microstructure in alloy 718. 737–750.

[6] Smith, G. D., & Patel, S. J. (2005). The role of Niobium in wrought Precipitation-hardened Nickel-base alloys.

[7] Hassan, B., & Corney, J. (2017). Grain boundary precipitation in Inconel 718 and ATI 718Plus.

[8] Wlodek, S. T., & Field, R. D. (1994). The Effects of Long Time Exposure on Alloy 718.

[9] Sabol, G. P., & Stickler, R. (1969). Microstructure of Nickel-Based Super-alloys.

[10] Sundararaman, M., Division, M. S., & Atomic, B. (n.d.). The stability of gamma double prime.

[11] Jambor, M., Bok, O., Nový, F., Trško, L., & Belan, J. (2017). Phase Transformations in Nickel base Super-alloy Inconel 718 during Cyclic Loading at High Temperature. 15, 2013–2016.

[12] Pineau, D. A. (1973). Morphology of Y’ and Y" Precipitates and Thermal Stability of Inconel 718 Type Alloys. 4(January).

[13] Deng, D. (2018). Additively Manufactured Inconel 718 : Microstructures and Mechanical Properties.

[14] Devaux, A., Naz, L., Molins, R., Pineau, A., Organista, A., & Uginet, J. F. (2008). Gamma double prime precipitation kinetic in Alloy 718. 486, 117–122.

[15] Nguyen, L., Shi, R., Wang, Y., & Graef, M. De. (2016). Acta Materialia Quantification of rafting of γ ′ precipitates in Ni-based super alloys. Acta Materialia, 103, 322–333.

[16] Rene, N., Rene, N., & Rene, N. (2003). Rafting in single crystal nickel-base super-alloys – An overview. 28(April), 115–128.

[17] Chang, S., Lee, S., & Huang, K. (2010). Influences of 00 and Precipitations on the Microstructural Properties of 718 Alloy through HIP, Solid-Solution, and Different Aging Heat Treatments. 51(9), 1683–1688.

[18] Segersäll, M. (2013). Nickel-Based Single-Crystal Super-alloys temperature properties.

[19] Ni based super alloys, Roger reed. (n.d.).

[20] Brooks, J. W., & Bridges, P. J. (1988). Metallurgical Stability of Inconel Alloy 718.

[21] Radavich, J. F. (1989). The physical Metallurgy of cast and wrought alloy 718.

[22] Lee, S., Takahashi, E., Nomura, N., & Chiba, A. (2005). Effect of Heat Treatment on Microstructure and Mechanical Properties of Ni- and C-Free Co – Cr – Mo Alloys for Medical Applications globular.

[23] Azadian, S. (2004). Aspects of Precipitation in the Alloy Inconel 718.

[24] Cristiane, K., Candioto, G., Caliari, F. R., & Nunes, C. A. (2015). Mechanical and Materials Engineering of Modern Structure and Component Design. 70, 293–300.

[25] Hwang, I. I. S., Ballinger, R. G., Morra, M. M., Tao, B., & Mathew, S. (n.d.). Improved Mechanical Properties of Alloy 718 by Anneal and Direct Aging Process for Nuclear Fusion Applications.

[26] Sauvage, X., & Mukhtarov, S. (n.d.). Aeronautical requirements for Inconel 718 alloy.

[27] Kracke, A. (2010). Super-alloy, the most successful alloy system of modern times - past, present and future.

[28] Andersson, J. (2012). Homogenization of Precipitation Hardening Nickel Based Super-alloys.

[29] Wang, C., & Li, R. (2004). Effect of double aging treatment on structure in Inconel 718 alloy. Journal of Materials Science, 39(7).

[30] Mills, W. J. (1991). Effect of Microstructural Fracture Toughness Variations of Wrought Alloy.

[31] Xie, X., Dong, J., Wang, G., & You, W. (2005). The effect of Nb, Ti, Al on the precipitation and strengthening behavior of 718 type super alloys. 3, 287–298.

[32] Maj, P., Adamczyk-Cieslak, B., Slesik, M., Mizera, J., Pieja, T., Sieniawski, J. Dudek, S. (2017). The Precipitation Processes and Mechanical Properties of aged Inconel 718 alloy after annealing. Archives of Metallurgy and Materials, 62(3), 1695–1702.

[33] Ghosh, S., Yadav, S., & Das, G. (2008). Study of standard heat treatment on mechanical properties of Inconel 718 using ball indentation technique. Materials Letters, 62(17–18), 2619–2622.

[34] Kishan, E. V. R., & Nagarajan, N. M. (2015). Strengthening of Forged Inconel Super alloy by Age Hardening Heat Treatment. 2(8), 387–391.

[35] Tucho, W. M., Cuvillier, P., Sjolyst-Kverneland, A., & Hansen, V. (2017). Microstructure and hardness studies of Inconel 718 manufactured by selective laser melting before and after solution heat treatment. Materials Science and Engineering A, 689(December 2016), 220–232.

[36] Xu, J., Huang, Z., & Jiang, L. (2017). Effect of heat treatment on low cycle fatigue of IN718 super alloy at the elevated temperatures. Materials Science and Engineering A, 690, 137–145.

[37] Garat, V., Deleume, J., Cloue, J.-M., & Andrieu, E. (2012). High Temperature Inter-granular Oxidation of Alloy 718. 559–569.

[38] Bor, H., Wei, C., Nguyen, H. T., Yeh, A., Kuo, C., & Engineering, A. (2010). Aging effect on the γ′ and γ″ precipitates of Inconel 718. 7th International Symposium on Super alloy 718 and Derivatives, 679–688.

[39] Thomas, A., El-Wahabi, M., Cabrera, J. M., & Prado, J. M. (2006). High temperature deformation of Inconel 718. Journal of Materials Processing Technology.

[40] Sindhura, D., Sravya, M. V., & Murthy, G. V. S. (2019). Comprehensive Microstructural Evaluation of Precipitation in Inconel. Metallography, Microstructure, and Analysis, (0123456789).

[41] Zhong, C., Gasser, A., & Kittel, J. (2016). Microstructures and tensile properties of Inconel 718 formed by high deposition-rate laser metal deposition. 022010.

[42] Korth, G. E., & Trybus, C. L. (1991). Tensile Properties and Microstructure of Alloy 718 Thermally Aged to 50,000 Hours. 437–446.

[43] Lee, S., Chang, S., Tang, T., Ho, H., & Chen, J. (2006). Improvement in the Microstructure and Tensile Properties of Inconel 718 Super alloy by HIP Treatment. 47(11), 2877–2881.

[44] Oyyaravelu, R., Felix, J., Kumar, R., & Jerome, S. (2018). Science Direct Effect of Heat Treatment on the Microstructure and Mechanical Properties of Inconel 718. Materials Today: Proceedings, 5(2), 7716–7724.

[45] Chang, K.-M., Lai, H.-J., & Hwang, J.-Y. (2012). Existence of Laves Phase in Nb-Hardened Super alloys. 683–694.

[46] Sjoberg, G., Ingesten, N. G., & Carlson, R. G. (n.d.). Grain Boundary delta-phase Morphologies, Carbides and Notch Rupture Sensitivity of Cast Alloy 718. 603–620.

[47] Liu, P., Sun, S., Xu, S., Cao, M., Hong, C., & Hu, J. (2018). Effect of Solid Solution + Double Ageing on Microstructure and Properties in the Layer by Layer of the Z-Y Interface of Inconel 718 alloys Fabricated by SLM 2 . Experimental Techniques. 21(6).

[48] Sohrabi, M. J., Mirzadeh, H., & Ra, M. (2018). Solidification behavior and Laves phase dissolution during homogenization heat treatment of Inconel 718 super alloy. 154(April), 235–243.

[49] Ling, L., Han, Y., Zhou, W. E. I., Gao, H., Shu, D. A., Kang, M., & Sun, B. (2014). Study of Micro-segregation and Laves Phase in INCONEL718 Super alloy regarding cooling rate during solidification.

[50] Xiao, H., Li, S., Han, X., Mazumder, J., & Song, L. (2017). Corresponding author at : State Key Laboratory of Advanced Design and Manufacturing for. Materials & Design.

[51] Petroni, S. (2007). Heat Treatment Effect on Multicomponent Nickel Alloys Structure. 189–193.

[52] Allvac, N. S. (2020). Structure stability study on a newly developed nickel-base super alloy—allvac ® 718plus TM. 179–191.

[53] El-bagoury, N., Group, C., & Arabia, S. (2011). Microstructure and Mechanical Properties of Aged Nickel Base Super alloy. 3(2), 266–276.

[54] Suresh, S. (n.d.). Elastic-Plastic Fracture Mechanics.

[55] Schirra, J. J. (2012). Effect of Heat Treatment Variations on the Hardness and Mechanical Properties of Wrought Inconel 718. 431–438.

[56] Raghavan, S., Zhang, B., Wang, P., Sun, C. N., Nai, M. L. S., Li, T., & Wei, J. (2017). Effect of different heat treatments on the microstructure and mechanical properties in selective laser melted INCONEL 718 alloy. Materials and Manufacturing Processes, 32(14), 1588–1595.

[57] Rao, G. A., Kumar, M., Srinivas, M., & Sarma, D. S. (2012). Effect of Solution Treatment Temperature on the Microstructure and Tensile Properties of P/M (HIP) Processed Superalloy INCONEL 718. 605–616.

[58] Popovich, V. A., Borisov, E. V., Popovich, A. A., Sufiiarov, V. S., Masaylo, D. V., & Alzina, L. (2017). Functionally graded Inconel 718 processed by additive manufacturing: Crystallographic texture, anisotropy of microstructure and mechanical properties. Materials and Design, 114, 441–449.

[59] Mignanelli, P. M., Jones, N. G., Pickering, E. J., Messé, O. M. D. M., Rae, C. M. F., Hardy, M. C., & Stone, H. J. (2017). Scripta Materialia Gamma-gamma prime-gamma double prime dual-super lattice super alloys. Scripta Materialia, 136, 136–140.